Attainable Reaction and Separation Processes from a Superstructure-Based Method

Patrick Linke and Antonis Kokossis
Centre for Process and Information Systems Engineering, School of Engineering, University of Surrey, Guildford, Surrey, GU2 7XH, U.K.

Generic technology for the synthesis and optimization of integrated reaction and separation systems uses rich superstructure formulations comprising two types of generic synthesis units with flexible representation modes. A reactor/mass exchanger unit enables a detailed representation of the reaction and mass exchange phenomena. A conceptual representation of separation systems is facilitated through separation task units. All possible process designs featuring reaction, reactive separation, and separation are embedded in the superstructure formulations as combinations of generic units and their features. The design options are explored using stochastic optimization techniques suitable for this class of problems. The flexible representation framework enables technology applications to general process design, as well as design subproblems including reactor and reactive separator design. Four case studies demonstrate the ability of the methodology to address a wide variety of process systems and to deliver design novelty.

Introduction

The development of process synthesis tools has mainly been confined to isolated sub-systems, which are typically reactor networks, separation systems, and energy systems. The literature on synthesis methods for these systems is immensely rich, so that a review is not attempted here. There are strong and complex interactions between the individual sub-systems, in particular between the reaction and the separation systems. Full exploitation of these interactions is difficult to impossible with available synthesis tools developed to address only the sub-systems. The development of systematic synthesis tools for integrated reaction and separation systems has received considerably less attention. Again, the developments have mainly been confined to sub-problems of integrated reaction and separation problems, such as reactor-separator recycle and specific reactive separation systems.

Reactor-separator-recycle process synthesis approaches include the work of Kokossis and Floudas (1991). They were the first to present a general superstructure formulation accounting for CSTRs and PFRs with side streams to exist in all possible combinations in the reaction section. The problem was formulated as a MINLP with the existence of reactors and sharp-split separators being discrete decisions. Smith and Pantelides (1995) later proposed the use of more detailed process models in the MINLP formulation in conjunction with process units that do not perform predefined tasks. Dynamic programming techniques were applied by Fraga (1996) to a discretized reactor-separator synthesis problem. The presented formulations for reactor-separator-recycle systems address problems with only one fluid phase. That is why they cannot account for reactive separation options.

Mainly graphical techniques have been presented for the synthesis of reactive separation systems. Such methods aim at producing feasible design candidates and are available for reactive distillation, reactive extraction, and reactive crystallization problems (Barbosa and Doherty, 1988; Hauan et al., 2000a,b; Nisoli et al., 1997; Ng and Samant, 1998; Ng and Berry, 1997; Okasinski and Doherty, 1998). Although very useful for illustration purposes and to initialize rigorous simulations, the methods fail to provide any systematic comparison of design options. In contrast to this, Ciric and Gu (1994) adopt an optimization-based approach. They formulate a reactive distillation column as a MINLP with the number of stages and the feed locations being the structural decision variables. Recently, Cardoso et al. (2000) subjected the same representation to stochastic optimization in the form of simulated annealing. In the synthesis of reactor networks, Bala-

Correspondence concerning this article should be addressed to A. Kokossis.

krishna and Biegler (1993) and Lakshmanan and Biegler (1996) accounted for intermediate separation by introducing a discretized reaction-separation model and a mass integrated reactor network, respectively. Stein et al. (1999) propose superstructure networks employing two-phase reactor-condenser elements for vapor-liquid systems formulated as NLPs, that is, they do not systematically account for discrete design decisions. The assumption of well-mixed reaction elements offers only limited representation potential for multiphase reacting and reactive separation systems. Even some conventional multiphase mixing and contacting patterns cannot be captured by the synthesis elements or their combinations. The same limitation is observed in the approach of Papalexandri and Pistikopoulos (1996), who propose the exhaustive connection between postulated units for reaction and separation formulated as MINLPs. The method has taken up applications in reactive and reactor/separation system synthesis (Ismail et al., 1999a, 2001), as well as homogeneous azeotropic distillation design (Ismail et al., 1999b). The approach requires to cope with large MINLP formulations that include nonlinearities of the most general type.

This work introduces a general framework for the synthesis and optimization of processes involving reaction and separation. The scheme employs rich and inclusive superstructure formulations of two different types of synthesis units and stream networks that allow for a conceptual, as well as a rigorous, representation of the chemical and physical phenomena encountered in general reaction and separation systems. Stochastic search techniques are applied to identify performance targets and a set of near-optimal flow schemes from the superstructures that closely achieve the targets. The case studies demonstrate the ability of the design tool to address a wide variety of process systems and to obtain novel designs for these systems. The design candidates provided by the tool give insights into the problem that are found to enhance the understanding of the process system, which allows to support the decision-making in subsequent design efforts.

Design Problem and Synthesis Approach

Potentially beneficial interactions between reaction and separation are manifold and can result from either separation within the reaction zones of the process (reactive separation systems), appropriate combinations of separate reaction and separation equipment (reactor-separator systems), or from a combination of the above. The realization of reactive separation options requires the introduction of mass separating options into the reaction equipment, and results in additional phases or states that need to be considered in the process synthesis. Common examples are the introduction of solvents (reactive extraction, reactive absorption), stripping agents (reactive distillation), solids (reactive crystallization), or diffusion barriers (membrane reactors). In general reactor-separator systems, a number of separation tasks exist that enable the generation of intermediates or products of performance enhancing nature in the context of a general reacting system. A general synthesis problem statement for this type of system is given as follows: *Given a set of raw materials, the reaction path and kinetics, the thermodynamic property data, the desired product specifications, and a performance measure determine the performance target of the system along with a set of design options with performances approaching the targets.*

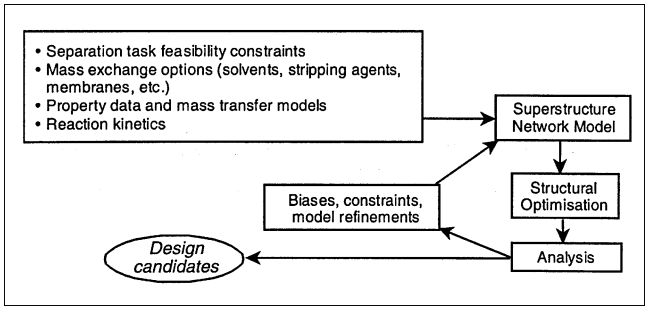

Figure 1. Synthesis strategy.

This article addresses the automated synthesis of process configurations that exploit interactions between reaction and reactive separation such that a specified process performance measure is optimized. We propose the synthesis strategy illustrated in Figure 1. The available process design information for candidate reactive separation and mass exchange operations is incorporated into generic synthesis unit models. Superstructures of these generic units are then formulated and the performance targets, as well as a set of design candidates, are obtained subsequently via robust stochastic optimization techniques. The synthesis strategy allows for iterations to incorporate the insight gained during the synthesis process. Reasons for iterations are the identification of additional problem constraints, the removal of process units without positive impact on the system performance, or the inclusion of refined process models. Such refinements might result from the limited validity of the available reaction models in optimal design regions so that the model trade-offs might not reflect the real system trade-offs. Refined process models, valid in the operation regions identified to be of interest, may introduce additional model nonlinearities or an additional set of reactions and components. The proposed synthesis technology is required to address such additional model complexity.

Process Unit Representation

As mentioned above, generic synthesis units are the building block of the superstructure representations. The proposed methodology utilizes two types of generic units: the reactor/mass exchanger (RMX) and the separation task (ST) unit. This section describes the synthesis units, the generation of the superstructures, and the optimization technology employed to optimize them.

Generic reactor/mass exchanger unit

The underlying phenomena exploited in chemical process design are reaction, heat, and mass exchange. They are generally exploited simultaneously (nonisothermal multiphase reactors and reactive separators), in combinations (nonisothermal homogeneous reactors and mass exchangers), or in isolation (isothermal reactors and mass exchangers, heat exchangers), depending on the particular system under investigation and the location of the operation within the flowsheet. This work employs the generic RMX unit for a flexible and

compact synthesis representation of the possibilities for phenomena exploitation in processing equipment. The RMX unit follows the *shadow compartment* concept developed for non-isothermal multiphase reactor network synthesis (Mehta and Kokossis, 1997, 2000). The unit consists of compartments in each phase or state present in the system under investigation. The streams processed in the different compartments of the generic unit can by definition exchange mass across a physical boundary, which can either be a phase boundary or a diffusion barrier. Each compartment features a superset of mutually exclusive mixing patterns through which a compact representation of all possible contacting and mixing pattern combinations between streams of different phases can be realized.

The RMX unit is illustrated in Figure 2 for a system featuring two phases or states. Each compartment receives inlet streams within its state and corresponds with the compartments in the other states via diffusional mass exchange links across the state boundaries. The effluents from the compartments either leave the unit or are recycled within the RMX unit. Recycles can be present within a given state or across the state boundaries if technically possible, such as by reboiling, condensing, throttling, or compression. Throughout this work, all states that can receive streams from a reference state are termed attainable states to the reference state. Mutually exclusive mixing options considered for the compartments include well-mixed and segregated flow. In order to avoid a mathematical model with both differential and algebraic equations, segregated flow behavior is approximated with a serial arrangement of well-mixed units of equal volume with the resulting cell model consisting of only algebraic equations. The mixing representation inside a compartment is shown in Figure 2. In each compartment, all inlet streams are connected to all mixers prior to the sub-units. Each sub-unit effluent stream is split and connected to the subsequent sub-unit, as well as the final product mixer of the compartment. The recycle streams from the final product splitter distribute among all well-mixed units employed in the compartments of the attainable states.

Let $S=\{s_1, s_2, ...,s_n\}$, $n \in \mathfrak{N}$ be the set of fluid phase states of the system and $CP^s=\{cp_1, cp_2, ...,cp_n\}$, $n \in \mathfrak{N}$ be the set of components that are present in state s of the RMX unit rm under consideration. Each compartment in a given state features a set of inlet streams $F^s=\{f_1, f_2, ..., f_n\}$, $n \in \mathfrak{N}$, and a set of well-mixed sub-units $SK^s=\{sk_1, sk_2, ...,sk_n\}$, $n \in \mathfrak{N}$. Inlet stream candidates include raw material streams and effluents of other units embedded in the superstructure as described in the next section. Set $S_s^T=\{s_1, s_2, ...,s_p\}$, $S_s^T \subseteq S$, contains the attainable states to s (note that this set includes state s itself). Let variables $FF_{s,f,cp}$ and $OUTR_{s,rm,cp}$ denote the flow rates of component cp in feed f and the product of the compartment in phase s, respectively.

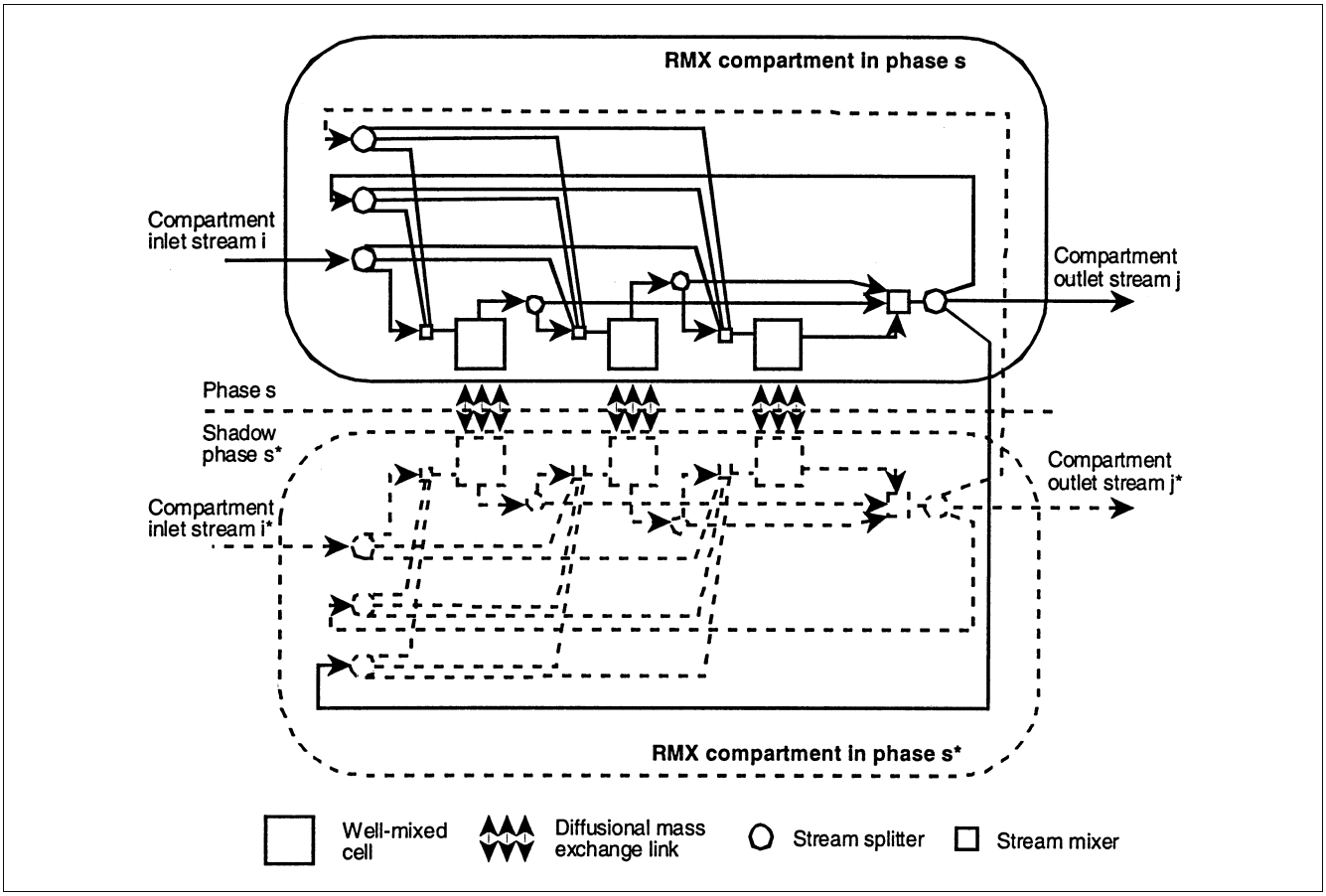

Figure 2. Reactor/mass exchanger unit.

$OUTSK_{s,rm,sk,cp}$ represents the flow rate of component cp in phase s at the outlet of each sub-unit sk, whereas $INR_{s,rm,sk,cp}$ denotes the flow rate of component cp entering the sub-unit. $FSF_{s,f,sk}$ denotes the fractions of the feed flow rates $FF_{s,f,cp}$ entering the sub-unit s. $SKP_{s,fm,sk} \in [0,1]$ represents the fraction of $OUTSK_{s,rm,sk,cp}$ entering the compartment product. The product recycle fraction in state s to sub-units sk in phase $s^* \in S_s^T$ is denoted by $SRR_{s^*,s,rm,rm,sk}$. The mass-transfer rate of component cp from sub-unit sk in phase s^* to the corresponding sub-unit in phase $s \in S \setminus \{s^*\}$ is denoted $MTR_{s^*,s,rm,sk,cp}$. $RXR_{s,rx,rm,sk}$ is the specific reaction rate of reaction rx in the reactive phase s, and $\nu_{s,rx,cp}$ is the stoichiometric coefficient for component cp in reaction $rx \in RX$. Additionally, $V_{s,rm}$ is the volume of the RMX unit and $\epsilon_{s,rm,sk}$ is the holdup of state s in sub-unit sk. The following material balances describe the RMX compartments ($|X|$ denotes card X):

(a) Balances for each mixer prior to the sub-units

$$\sum_{f \in F} FF_{s,f,cp} FSF_{s,f,sk} + PREV_{sk} + \sum_{s^* \in S_s^T} OUTR_{s^*,rm,cp} SRR_{s^*,s,rm,rm,sk} - INR_{s,rm,sk,cp} = 0 \quad \forall (sk \in SK, s \in S, cp \in CP) \quad (1)$$

where $PREV_{sk=1} = 0$ and $PREV_{sk \in SK_{s,rm} \setminus (1)} = OUTSK_{s,rm,sk-1,cp}(1 - SKP_{s,rm,sk-1})$.

(b) Balances for the sub-units

$$INR_{s,rm,sk,cp} + \sum_{rx \in RX_{s,rm}^A} \nu_{s,rx,cp} RXR_{s,rx,rm,sk} \frac{\epsilon_{s,rm,sk} V_{s,rm}}{|SK_{s,rm}|} + \sum_{s^* \in S \setminus \{s\}} MTR_{s^*,s,rm,sk,cp} - OUTSK_{s,rm,sk,cp} = 0 \quad \forall (s \in S, sk \in SK, cp \in CP) \quad (2)$$

(c) Balances of the final product mixer

$$\sum_{sk \in SK_{s,rm}} OUTSK_{s,rm,sk,cp} SKP_{s,rm,sk} - OUTR_{s,rm,cp} = 0 \quad \forall (s \in S, cp \in CP) \quad (3)$$

(d) Constraints on split fractions

$$\sum_{s^* \in S_s^T} SRR_{s^*,s,rm,rm,sk} - 1 < 0 \quad \forall (sk \in SK, s \in S) \quad (4)$$

$$\sum_{sk \in SK} FSF_{s,f,sk} - 1 = 0 \quad \forall (f \in F, s \in S) \quad (5)$$

Equations 1 to 5 represent a well-mixed compartment in state s for $|SK^s| = 1$ and an approximated segregated flow compartment for $|SK^s| > 1$. Mass-transfer rates $MTR_{s^*,s,rm,sk,cp}$ are calculated as functions of mixing patterns and flow directions in the compartments of states s and s^* according to the shadow compartment concept (Mehta and Kokossis, 1997, 2000; Mehta, 1998). The existence of mass-transfer links between the different compartments of the RMX units is a degree of freedom for optimization, and mass exchange interactions between the compartments in the different states present can be established or removed. This allows for decoupling of the reaction and mass-transfer phenomena in the system between a pair of compartments in states t and q by setting $MT_{q,t,s,c} = MT_{t,q,s,c} = 0$ in Eq. 2. Isolation of states is an important feature of the unit representation, as it might only be beneficial to introduce additional states to parts of the reaction-separation network. Decisions on the existence of catalyzed reactions are introduced to the RMX representation, allowing to account for the absence of catalysts in the reacting phases by setting $RX_{q,c} = 0$ in Eq. 2. Temperature effects are accounted for in the compartment models in accordance with the profile-based and the unit-based synthesis approaches presented by Mehta and Kokossis (2000). In the profile-based approach, temperature control profiles are imposed on the compartments the shape of which is a degree of freedom for optimization. This allows to determine the optimal temperature policies inside the processing units without the need for detailed consideration of individual heat-transfer mechanisms. For a more detailed design, a rigorous unit-based approach is utilized to account for temperature effects, by solving the energy balances of the units along with the mass balances of Eqs. 1–5. The compartments are represented by sections of adiabatic operation. Temperature control units are introduced that allow for the representation of all possible direct and indirect heat-transfer options. For details on the implementation of the profile-based and the unit-based approaches, we refer to Mehta and Kokossis (2000).

The different mixing patterns in the compartments, the existence of mass-transfer links, and the presence of catalysts enables to represent a variety of processing alternatives by a *single* generic unit. For a vapor-liquid-liquid system featuring reactions in one heterogeneously catalyzed liquid phase, the design alternatives in terms of phase interactions are shown in Figure 3. The compartments in each phase feature well-mixed and segregated flow units and each illustrated case represents itself a number of design alternatives resulting from different possible combinations of mixing patterns and flow directions in the different phases. If all mass-transfer links are deactivated, the RMX unit reduces to a homogeneous reactor, as shown in Figure 3a. Deactivated mass-transfer links to one phase transform the unit into a vapor-liquid reactor or an extractive reactor (Figures 3b and 3c). Removal of the catalyst realizes a vapor-liquid or a liquid-liquid mass exchanger (Figures 3d and 3e). If all mass-transfer links are active, the RMX unit represents a gas-liquid-liquid reactor (Figure 3f) or vapor-liquid-liquid mass exchanger for the case that no catalyst is present in the system. For systems with multiple states, a single RMX unit can represent more than one physically distinct unit simultaneously. For instance, the homogeneous reactor and the absorber/stripper shown in Figure 3 can coexist. The recycle options among compartments in the attainable states allow for additional design options to be captured by the RMX unit. Figures 3g–3j show the special cases that exist for the vapor-liquid mass exchanger of Figure 3d. Without recycles to attainable states, the unit represents an absorber (Figure 3g). A vapor recycle to the liquid phase results in a rectifier (Figure 3h), a liquid recycle to the vapor phase represents a stripper (Figure 3i), and a vapor and a liquid recycle results in a distil-

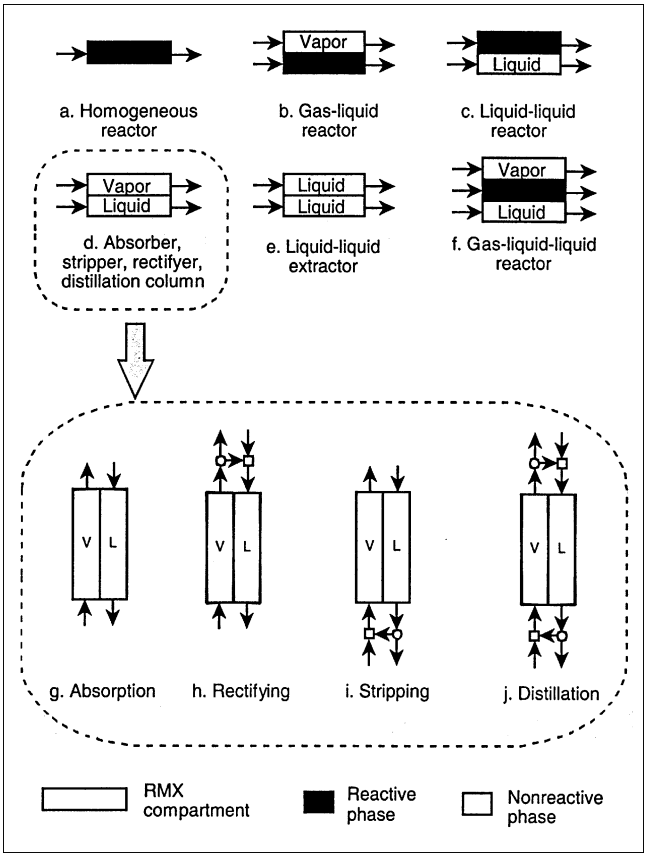

Figure 3. RMX design alternatives for a gas-liquid-liquid system with one reactive liquid phase.

lation column (Figure 3j). The recycle streams across the state boundary represent a condenser and a reboiler, respectively.

Separation task unit

In contrast to the rigorous representation of reaction and mass-transfer phenomena by RMX units, the separation task units (STU) represent venues for composition manipulations of streams without the need for detailed physical models. In accordance with the purpose of any separation system, the separation task units generate a number of outlet streams of different compositions by distributing the components present in the inlet stream among the outlet streams.

The separation task units and its inlet, as well as outlet streams, belong to the same state of the system under consideration. The unit is illustrated in Figure 4. Let $SC = \{sc_1, sc_2, ..., sc_r\}$, $r \in N$ be the set of components present in the processing state of the separation task unit and $NO = \{no_1, no_2, ..., no_s\}$, $s \in N$, $s > 1$ be the number of outlet streams leaving the unit. The inlet flow matrix $\underline{\underline{IF}} = \text{diag}(if_1, if_2, ..., if_r)$, $\underline{\underline{IF}} \in \Re^{r \times r}$, defines the molar component flow rates entering the unit. The outlet flow matrix $\underline{\underline{OF}} = (of_{r,s})$, $\underline{\underline{OF}} \in \Re^{r \times s}$ is defined by Eq. 6

$$\underline{\underline{OF}} = \underline{\underline{IF}} \cdot \underline{\underline{CD}} \tag{6}$$

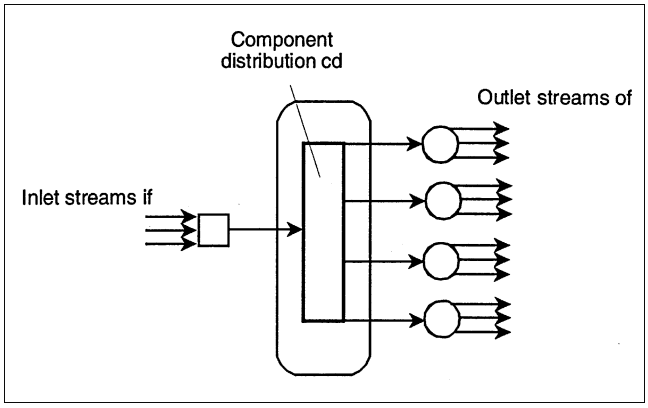

Figure 4. Separation task unit.

where $\underline{\underline{CD}} = (cd_{r,s})$, $\underline{\underline{CD}} \in \Re^{r \times s}$, $cd_{sc,no} \in [0,1]$ is the component distribution matrix. The sth column of the outlet flow matrix corresponds to the molar flow vector of the sth outlet stream of the separation task unit. The component distribution split fractions are constrained by Eqs. 7 and 8

$$\sum_{s \in NO} cd_{r,s} - 1 = 0 \quad \forall r \in SC \tag{7}$$

$$\sum_{r \in SC} \sum_{s \in NO} cd_{r,s} - r_{\max} = 0. \tag{8}$$

Note that, independent of the component distribution policies, the generic unit is described by linear mass balances

$$if_s - \sum_{r \in NO} of_{s,r} = 0 \quad \forall s \in SC \tag{9}$$

The component distribution matrix determines the functionality of the separation task unit. Let the set $O = \{o_1, o_2, ..., o_\upsilon\}$, $\upsilon \in N$, denote the separation processes that can be associated with the unit. For each process, a set of component lumps $LC_o = \{LSC_{o,1}, LSC_{o,2}, ..., LSC_{o,3}\}$, each comprised by subsets of components $LSC_{o,s} = \{lsc_{o,s,1}, lsc_{o,s,2}, ..., lsc_{o,s,u(s)}\}$, $u(s) \in N$, $lsc \in SC$, with common separation properties is defined such that

$$\cup_{u=1}^{u_{\max}} LSC_{o,u} = SC \quad \forall o \in O \tag{10}$$

In case all components are considered separable, the set of lumped components is identical to the component set SC. Separations between components of the same lump are not considered feasible. Consequently, for each lump $LSC_i \in LC$

$$cd_{isc,s} - cd_{jsc,s} = 0 \quad \forall s \in NO, isc, jsc \in LSC_i \tag{11}$$

Each outlet stream is assigned a set of $OC_s = \{oc_{s,1}, oc_{s,2}, ..., oc_{s,o(s)}\}$, $o(s) \in N$, $OC_s \subset LC$ component lumps. The separation task unit generates a maximum of $s_{\max}$ outlet streams by performing a set of separation tasks $T = \{t_1, t_2, ..., t_u\}$, $u \in N$. A number of separation tasks s partition the set of component lumps into $(s+1)$ subsets, which are assigned to the

$(s+1)$ outlet streams. The separation task units accommodates for the different synthesis aims in the screening and design stages outlined in the previous section by different levels of component distribution and separation task constraints.

The separation task unit can facilitate the representation of separation tasks that can be performed using particular separation processes. The possible distribution policies of component lumps to the outlet streams are constraint by the separation orders of the separation process. Let the function $f_{EP}(LSC)$: $G \rightarrow \Re$ return the physical property values that define the separation order for the component lumps of the unit operation considered (such as volatilities in case of distillation). Let the set LC be in descending order of separation such that $f_{EP}(LSC_1) > f_{EP}(LSC_2) > ... > f_{EP}(LSC_s)$. Component lump distribution policies are constraint such that the separation tasks can partition the set of component lumps into subsets containing adjacent elements of LC only.

Let task t partition the set of lumped components LC into subsets $A = \{a \in LC: f_{EP}(a) \geq f_{EP}(LSC_t)\}$ and $B = \{b \in LC: f_{EP}(b) < f_{EP}(LSC_t)\}$. Then, with the task set T in ascending order, the tasks $t_u \in T$ assign the components to the $(u_{\max}+1)$ outlet streams according to

$$\cup_{s=t_{u-1}+1}^{t_u} LSC_s = OC_{t_u} \tag{12a}$$

$$\cup_{s=t_{u_{\max}}+1}^{s_{\max}} LSC_s = OC_{t_{u_{\max}}+1} \tag{12b}$$

The key component lumps of the separation task t_u are LSC_{tu} and LSC_{tu+1}. If sharp separations are considered, the component distribution fractions are assigned according to Eq. 12. Alternatively, the key components can be allowed to distribute among outlet streams t_u and t_{u+1}, while satisfying Eq. 11. Nonsharp separations arising from operational constraints on the separation tasks can easily be accomplished. In the case of azeotrope formation, the component distribution fractions are constrained according to the corresponding compositions. Consider a separation task A(B)/(A)B where A and B form an azeotrope of composition x_{ic}^* and mixture AB leaves via effluent stream io and component A or B is obtained from effluent stream jo of the separation task unit. Then, the component distribution fractions are expressed as the following functions of the molar inlet flows

$$cd_{A,io} = \min\left(1, \frac{IF_B x_A^*}{IF_A(1-x_A^*)}\right),\ cd_{A,io} = 1 - cd_{A,jo};$$

$$cd_{B,io} = \min\left(1, \frac{IF_A x_B^*}{IF_B(1-x_B^*)}\right),\ cd_{B,io} = 1 - cd_{B,jo}.$$

In this case, the component distribution fraction is a function of the molar inlet flows and the mass balance of the separation task unit becomes nonlinear. Note that the purpose of the separation task unit is to provide for a conceptual representation of separation options and that a detailed representation of azeotropic systems can be accomplished with the use of RMX units and their combinations.

The separation task unit performs a set of feasible separation tasks according to the separation order to define a set of outlet streams. Depending upon the order in which the tasks are performed, a variety of processing alternatives exist for a single unit. In the following, it is illustrated how the separation task unit can be associated with processing equipment under the assumption that each separation task is performed by a simple "one feed–two products" separator and only arrangements of separators in series/parallel are considered. Similarly, the task vector can be associated with complex separations by adopting the representation of Shah and Kokossis (2002).

Let $\underline{T}$ be the s-dimensional task vector where each row is represented by one $t_s \in T$ without repetition of elements. With the convention that task t_{s-1} is performed before task t_s, the task vector defines a separator sequence. Consider a unit separating an inlet stream containing $LC = \{A, B, C, D, E, F, G\}$ by performing a set of tasks $T = \{1, 3, 4, 6\}$. Then, the task vector $\underline{T} = [1, 3, 4, 6]$ corresponds to the direct sequence shown in Figure 5a. The 13 alternative designs are realized by interchanging the rows of the task vector. For instance, interchanging rows 1 and 3 results in $T = [4, 3, 1, 6]$, which represents the sequence shown in Figure 5b. Interchanging the rows of the task vector allows to transform the separation sequence. Let k and k^*, $k > k^*$ be the ranks of the tasks to be interchanged in $\underline{T}$. Then, the resulting separation sequence is distinct if there exists a task of intermediate rank such that $\{t_j \in T: (t_{k^*} < t_j < t_k) \vee (t_{k^*} > t_j > t_k), k^* < j$

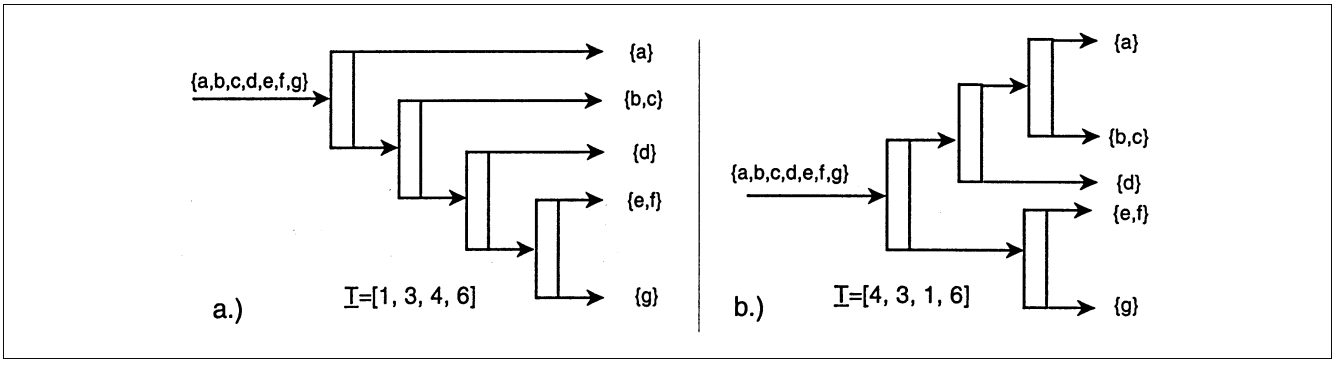

Figure 5. Generation of alternative separation sequences.

$< k\} \neq \{\ \}$. The separation process to be associated with the separation task unit, and the number of separation tasks, as well as their arrangements in the task vector, are decision variables for optimization.

Process System Representation and Optimization

Superstructure representation

The generic synthesis units presented above and their combinations allow for representation of all sections of general steady-state processes involving reaction and separation, that is, reaction sections, reactive separation sections, mass exchange sections, and sections performing separation tasks. The aim of the superstructure network generations is to provide for a venue that enables the simultaneous exploration of the functionalities of the different synthesis units along with all possible interactions among them. A number of synthesis units and a complete stream network are required to capture all the different design options that exist for a process. Novelty is accounted for in the superstructures, as the representations are not constraint to conventional process configurations, but instead include all possible novel combinations of the synthesis units.

The superstructures feature a number of generic RMX and separation task units, as well as raw material sources and product sinks, the interconnections among which are realized by two types of stream networks:

(a) *Intraphase streams* establish connections between the synthesis units, products, and raw materials of the same state; and

(b) *Interphase streams* establish those connections across the state boundaries, that is, the source and sink of such a stream belong to attainable states.

To describe the superstructure network generation, we define the following sets and subsets associated with the phases or states, synthesis units, the process streams, the raw materials and the products.

$S = \{s \text{ is a state}\}$
$RM = \{rm \text{ is a reactor/mass exchanger unit}\}$
$ST_s = \{st \text{ is a separation task unit in state } s \in S\}$
$F_s = \{f \text{ is a raw material source in state } s \in S\}$
$P_s = \{p \text{ is a product in state } s \in S\}$
$SP_s = \{sp \text{ is a splitter in state } s \in S\}$
$MI_s = \{mi \text{ is a mixer in state } s \in S\}$
$CP_s = \{cp \text{ is a component in state } s \in S\}$
$RX_s = \{rx \text{ is a reaction in state } s \in S\}$
$SO_{s,st} = \{so \text{ is an outlet of unit } st \in ST_s \text{ in state } s \in S\}$
$SK_{s,rm} = \{sk \text{ is a well-mixed sub-unit in the compartment in phase } s \in S \text{ of } rm \in RM\}$
$S^T_{s^*} = \{s | s \in S \text{ is an attainable state for } s^* \in S\}$
$SP^F_{s,f} = \{sp | sp \in SP^A_s \text{ splits a raw material stream } f \in F_s\}$
$SP^{RM}_{s,rm} = \{sp | sp \in SP^A_s \text{ splits the outlet of unit } rm \in RM\}$
$SP^{IRM}_{s,rm,sk} = \{sp | sp \in SP^A_s \text{ splits the outlet of sub-unit } sk \in SK_{s,rm} \text{ of } rm \in RM\}$
$SP^{ST}_{s,st,so} = \{sp | sp \in SP^A_s \text{ splits outlet so} \in SO_{s,st} \text{ of unit } st \in ST_s\}$
$SP^P_{s,p} = \{sp | sp \in SP^A_s \text{ splits a product stream } p \in P_s\}$
$MI^{RM}_{s,rm,sk} = \{mi | mi \in MI^A_s \text{ is a mixer prior to sub-unit } sk \in SK_{s,rm} \text{ of } rm \in RM\}$
$MI^{PRM}_{s,rm} = \{mi | mi \in MI^A_s \text{ is a final product mixer of } rm \in RM\}$
$MI^{ST}_{s,st} = \{mi | mi \in MI^A_s \text{ is a mixer prior to unit } st \in ST_s\}$
$MI^P_{s,p} = \{mi | mi \in MI^A_s \text{ is a mixer of product } p \in P_s\}$
$CP^P_{s,p} = \{cp | cp \in CP \text{ is a component allowed in product } p \in P_s\}$
$CP^F_{s,f} = \{cp | cp \in CP \text{ is a component in } sp \in SP^F_{s,f}\}$
$CP^{RM}_{s,rm} = \{cp | cp \in CP \text{ is a component in the outlet of } sp \in SP^{RM}_{s,rm}\}$
$CP^{ST}_{s,st,so} = \{cp | cp \in CP \text{ is a component in the outlet of } sp \in SP^{ST}_{s,st,so}\}$

In each state of the system, network superstructures are generated according to the following intraphase connectivity:

(1) Mixers $MI^{RM}_{s,irm,sk}$ are fed by streams originating from any splitters $SP^F_{s,f}$, $SP^{RM}_{s,jrm \neq irm}$ and $SP^{ST}_{s,st,so}$. Note that local recycles within the RMX units are already included into the unit representation.

(2) Mixers $MI^{ST}_{s,ist}$ receive streams from any splitters $SP^{RM}_{s,rm}$ and from all the splitters $SP^{ST}_{s,jst \neq ist,jso}$ that are separable according to $\{ic,jc \in CP^{ST}_{s,jst,jso}: ic \neq jc, ic \in CP^{ST}_{s,ist,iso}, jc \in CP^{ST}_{s,ist,kso \neq iso}\} \neq \{\ \}$. Similarly, streams originated from any splitters $SP^F_{s,if}$ are connected to $MI^{ST}_{s,ist}$ if $\{ic,jc \in CP^F_{s,if}: ic \neq jc, ic \in CP^{ST}_{s,ist,iso}, jc \in CP^{ST}_{s,ist,kso \neq iso}\} \neq \{\ \}$.

(3) Mixers $MI^P_{s,ip}$ receive streams originating from any splitters $SP^{RM}_{s,rm}$ that satisfy $CP^{RM}_{s,rm} \subseteq CP^P_{s,ip}$ and correspondingly from any splitters $SP^{ST}_{s,st,so}$ that satisfy $CP^{ST}_{s,st,so} \subseteq CP^P_{s,ip}$.

For a system with attainable states $s^* \neq sa \neq q$, the network superstructures additionally facilitate the following interphase connectivity:

(4) Mixers $MI^{RM}_{s,irm,sk}$ $MRMX_{q,ir,sc}$ receive streams originating from any splitters $SP^F_{s^*,f}$, $SP^{RM}_{s^*,jrm \neq irm}$ and $SP^{ST}_{s^*,st,so}$.

(5) Mixers $MI^{ST}_{s,ist}$ receive streams from any splitters $SP^{RM}_{s^*,rm}$ and from all the splitters $SP^{ST}_{s^*,jst,jso}$ that are separable according to $\{ic,jc \in CP^{ST}_{s^*,jst,jso}: ic \neq jc, ic \in CP^{ST}_{s,ist,iso}, jc \in CP^{ST}_{s,ist,kso \neq iso}\} \neq \{\ \}$. Similarly, streams originated from any splitters $SP^F_{s^*,if}$ are connected to $MI^{ST}_{s,ist}$ if $\{ic,jc \in CP^F_{s^*,if}: ic \neq jc, ic \in CP^{ST}_{s,ist,iso},\ jc \in CP^{ST}_{s,ist,kso \neq iso}\} \neq \{\ \}$.

The compositions of the streams remain unchanged upon state transition. The transfer of material across the state boundary potentially requires the addition or removal of energy to or from the interphase streams. In this case, an energy transfer unit such as a total reboiler or a total condenser, a throttle, or a compressor is associated with those mixers receiving a stream from a different state. For systems where components are present that are virtually involatile or incondensible at feasible operating conditions, the total operation of reboilers and condensers is an invalid assumption. It is important to point out that a temperature controlled RMX unit featuring well-mixed compartments in both attainable states enables the representation of partial reboilers and condensers. In this case a larger number of RMX units are to be included into the superstructure as the representation of processing options becomes less compact. The mathematical formulation of the superstructure model is presented in the Appendix.

Figure 6 illustrates three process configurations that are embedded in a two-phase superstructure network comprised of three RMX and three separation task synthesis units. A flow scheme featuring a reactive distillation arrangement with a homogeneous pre-reactor is shown in Figure 6a. The reactive distillation column is represented by two RMX units with plug-flow compartments in both phases and countercurrent

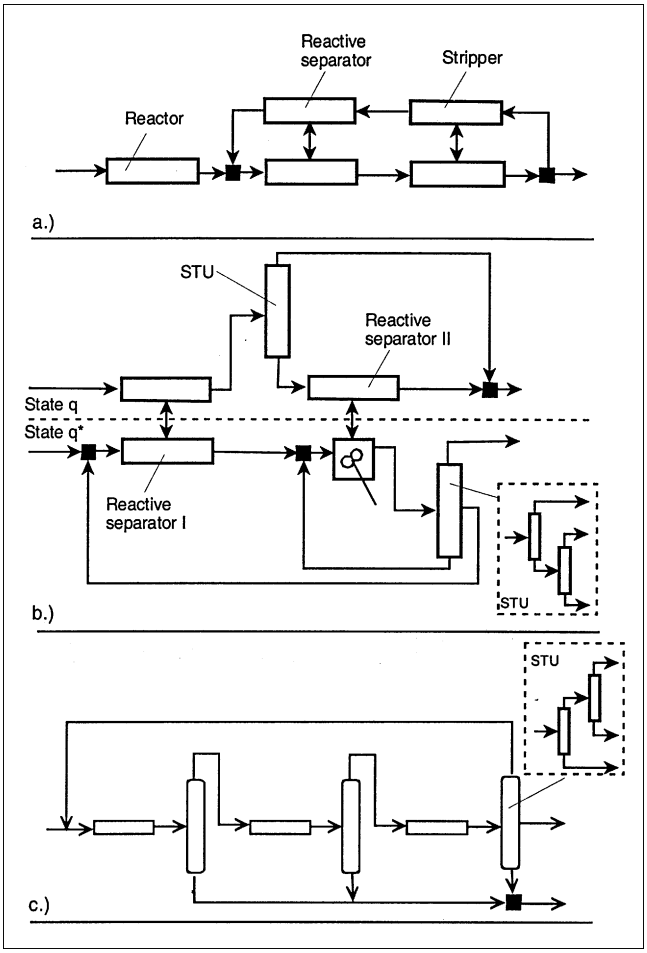

Figure 6. Novel and conventional designs embedded in the superstructure for a system with two fluid phases.

stream contacting. The design shown in Figure 6b does not feature any interphase connections, and reaction occurs in both RMX units. A separation task unit facilitates the intermediate separation of components in between the RMX units in state *s*. In state *s**, a plug-flow and a well-mixed RMX compartment are arranged in series followed by a separation task unit representing a separation sequence to separate the raw material from the product and the byproducts. Figure 6c shows a design of plug-flow reactors in serial arrangement with intermediate separations and a global recycle.

Clearly, the representation potential of a superstructure strongly increases with the number of synthesis units that are included in the formulation and a superstructure, which is too small, will result in missed opportunities. On the other hand, the addition of too many units unnecessarily increases the complexity of the formulation. How to determine the minimum number of synthesis units to be included into a superstructure for representation of all relevant design options is still an unanswered question in process synthesis and is certainly case-dependent. One should be aware that, if the initial superstructure does not contain the minimum number of synthesis units required for the representation of the optimal solution(s), the framework will lead to a sub-optimal design. Similarly, process features that are beyond the representation potential of (combinations of) the proposed synthesis units will not show in the superstructure and optimal designs containing those features cannot be obtained.

Superstructure optimization

The network optimization needs to exploit the structural, as well as the continuous, decisions within the network in order to arrive at optimal solutions. Due to the highly nonlinear and discrete nature of the general synthesis problem, the reaction and separation superstructures are optimized using stochastic search techniques in the form of simulated annealing (Kirkpatrick et al., 1983) in this work. SA does not deliver strict optima in a deterministic sense, but has been proven to converge statistically to the globally optimal domain (Aarts and van Laarhoven, 1985; Marcoulaki and Kokossis, 1999), that is, to the performance target of the system. The searches produce a multitude of stochastically optimal solutions with performances close to the target values.

The implementation of the SA procedure employs a set of moves that allows correspondence among all possible design states embedded in the network superstructure. The moves enable the contraction, expansion, and alteration of individual synthesis units and stream attributes of the design instances. Starting from an initial state, sequential transitions are considered towards improving, as well as disimproving, states with the probability of significant uphill excursions being reduced during the cooling of the system. Hence, the system is gradually forced towards states of better performance; however, on the path towards better performance, the system is allowed to attain inferior states. At each temperature, a number of random, reversible state transitions (homogeneous Markov chain) are performed to equilibrate the system. A *search heuristic* (acceptance criterion) exploits the knowledge of the performance of a current state, that of a potentially new state within its neighborhood, and the state of the search (the annealing temperature) to guide the transition towards the stochastic optimum. The search allows for transitions to disimproving states, thus enabling the system to escape from locally optimal states. This work employs the original Metropolis acceptance criterion (Metropolis et al., 1953) and

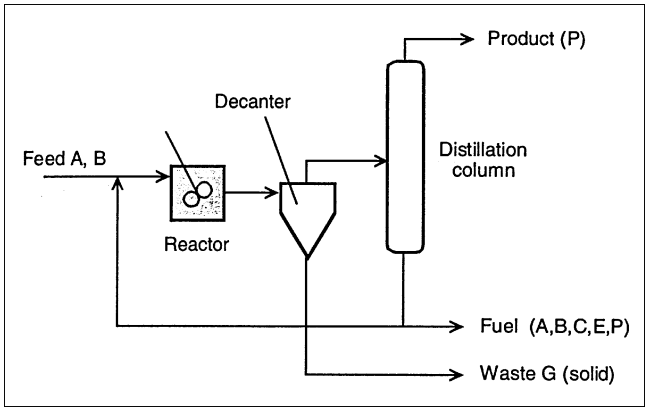

Figure 7. Conventional Williams-Otto process configuration.

the logarithmic cooling schedule suggested by Aarts and van Laarhoven (1985). Details on the implementation of the stochastic search algorithms will be presented in a future publication.

Examples

Example 1: the Williams-Otto flowsheeting problem

Novel designs for the Williams-Otto problem (Ray and Szekely, 1973) are sought. Figure 7 shows the conventional process configuration. The raw materials A and B are fed to a reactor where the following reactions occur

$$(1)\ \mathrm{A}+\mathrm{B}\rightarrow\mathrm{C}$$
$$(2)\ \mathrm{B}+\mathrm{C}\rightarrow\mathrm{P}+\mathrm{E}$$
$$(3)\ \mathrm{P}+\mathrm{C}\rightarrow\mathrm{G}$$

The reaction rates of components A, B, C, P, E, and G, respectively, are functions of the weight fractions X and given by the vector $\underline{R}(X)=[-k_1\ X_A\ X_B;\ -k_1\ X_A\ X_B-k_2\ X_B\ X_C;\ 2\ k_1\ X_A\ X_B-2\ k_2\ X_B\ X_C-k_3\ X_P\ X_C;\ k_2\ X_B\ X_C-0.5\ k_3\ X_P\ X_C;\ 2k_2\ X_B\ X_C;\ 1.5\ k_3\ X_P\ X_C]$ where $k_1=110.695$ wt. frac./h, $k_2=561.088$ wt. frac./h, and $k_3=1248.748$ wt. frac./h. The volatilities α_i of the components i in the system have the following descending order: $\alpha_P>\alpha_E>\alpha_C>\alpha_B>\alpha_A>\alpha_G$. As components E and P form an azeotrope, an amount of the desired product equivalent to at least 10% weight fraction of E is lost through the purge, which is used on-site as a fuel.

The objective of the synthesis exercise is to find the designs that maximize the annual profit of the process for a minimum production rate of 400 kg/h of component P. The profit function includes the product value and raw material costs, waste treatment cost, reactor capital, and operating cost, as well as the cost incurred by separation. A summary of the problem data is given in Table 1. Distillation enables separation of mixtures according to the order of volatilities and, hence, allows separation in support of the raw material and intermediate recovery. To avoid fouling, G needs to be decanted prior to the operation, which can be achieved at a low cost in a decanter. However, component P forms an azeotropic mixture with component E resulting in a loss of desired product to the low value fuel. A solvent is available that allows selective extraction of desired product P from the mixture. The following equilibrium relationship is assumed (Lakshmanan and Biegler, 1996): $x_{P,\mathrm{solvent}}=0.4x_{P,\mathrm{process-stream}}$. The maximum mass fraction of P in the solvent is $x^{\max}_{P,\mathrm{solvent}}=0.2$. The separation task units are allowed to perform splits between the key components of distillation, that is, the following separations can be performed by these units according to the order of component volatilities: *P/PE/C/B/A*. All splits performed by distillation are assumed to be equally difficult. The solvent introduces a second phase to the system. Thus, the RMX unit can take the functionality of a homogeneous reactor, a reactive extractor, or an extractor if the catalyst is absent. It is assumed that reactive extractors and extractors incur higher capital costs than a homogeneous reactor of identical volume. Superstructures featuring three RMX units, three separation task units in the reacting liquid phase, and one separation task unit for solvent regeneration are employed in the synthesis. Note that the two liquid phases are not miscible and the interphase connections are not considered.

Table 1. Problem Data for the Williams-Otto Process Synthesis Example

Parameter	Units	Value
Value of product P	\$/kg	0.2628
Value of byproducts A,B,C,P,E	\$/kg	0.0059
Cost of reactant A	\$/kg	0.02
Cost of reactant B	\$/kg	0.03
Cost of byproduct G (waste treatment)	\$/kg	0.01
Annual operating time	h/yr	8400
Capital expenditure amortization factor	1/yr	0.43
Reactor operation/flow through unit	\$/kg·yr	2.22
Reactor capital investment	\$/m^3	4800
Separation task costs*	C^{FIX}	C^{VAR}
Separation of G (decanter)	\$10,000	\$0.0001/kg
Distillation [Separations: $E(P)/P/C/B/A$]	\$200,000	\$0.001/kg
Solvent regeneration		\$0.001/kg
Equipment cost ratios**		
Homogeneous reactor (HR)	m^3_{HR}/m^3_{HR}	1
Reactive separator (RS)	m^3_{RS}/m^3_{HR}	10
Extractor (EX)	m^3_{EX}/m^3_{HR}	4

*Cost $=C^{\mathrm{FIX}}+F^{\mathrm{IN}}C^{\mathrm{VAR}}$.
**Base: homogeneous reactor volume.

Stochastic optimization yields a target performance of around \$433 k/yr for the system. Designs with performances close to the target can be grouped into two main categories

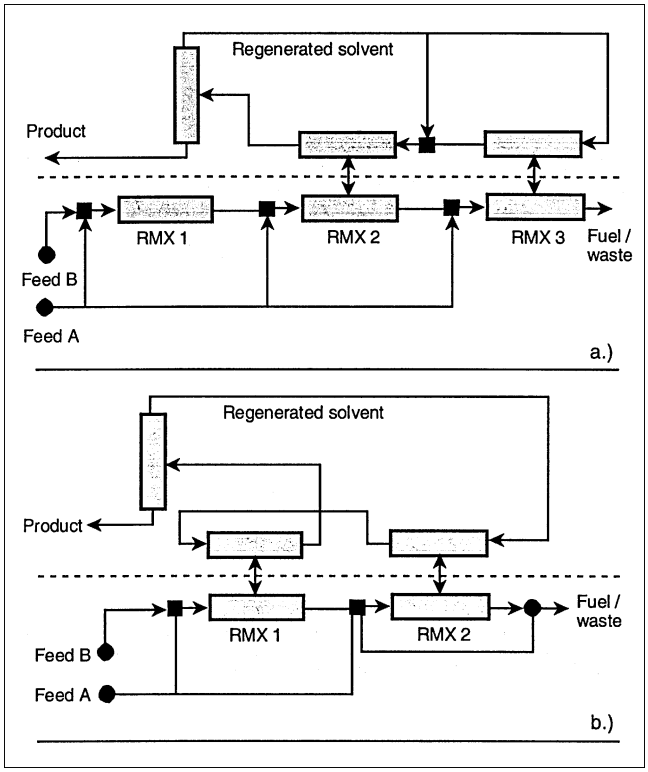

Figure 8. Reactive extraction processes from the design stage.

Table 2. Design Information for the Williams-Otto Process

Design of Figure		8a	8b	9a	9b
Objective	k$/yr	421	418	433	422
Unit volume (RMX 1)	L	28	101	160	13
Unit volume (RMX 2)	L	106	294	303	229
Unit volume (RMX 3)	L	280	n/a	n/a	190
Feed A	kg/h	565	552	468	483
Feed B	kg/h	1,140	1,069	905	927
Solvent from regeneration	kg/h	12,000	14,980	3,388	3,559
Product P	kg/h	400	400	400	400

according to their use of the solvent. Category 1 features reactive extraction designs and category 2 reactor-hybrid separation designs. Designs of the first category employ only RMX units featuring plug-flow compartments in the form of homogeneous reactors and reactive extractors. No separation tasks are utilized in the reactive phase, that is, extraction of the desired product P in the course of reaction is the only separation required to achieve the target. The optimal flow schemes feature two or three RMX units. Typical designs are shown in Figure 8. Additional design information is presented in Table 2. The compartments of the reactive liquid phase are arranged in series. Raw material B is fed to the first, whereas the raw material A is distributed among all compartments. When present in the optimal designs, homogeneous reactors are located prior to the reactive extractors (Figure 8a). The feeds to these units generally contain component B in excess. The solvent contacting pattern is mainly countercurrent, but combinations of cocurrent and countercurrent units are also observed (Figure 8b). The stochastic search has identified the reactive extraction designs, although their performances fall slightly short of the system's performance target (around 3%).

Designs of the second category feature RMX units in the form of homogeneous plug-flow reactors and countercurrent extractors, as well as a single separation task unit. Additionally, a number of flow schemes employ reactive extractors. Typical designs are illustrated in Figures 9a and 9b. Further design information is summarized in Table 2. The separation task unit facilitates a decanter for removal of solid waste G, as well as a distillation column for separation of product P and byproduct E from the raw materials and intermediates A, B, and C. In all designs proposed so far, the sloppy task $P/(P)E,C,B,A$ is performed by the distillation operation. In contrast, the novel designs utilize a distillation-extraction hybrid separation system for a complete recovery of valuable components P, A, B, and C. The solvent is used to extract the desired product P from the distillation column overheads in a countercurrent contractor. Only component E and a small fraction of P ($< 0.5\%$) are present in the fuel stream. The bottoms of the distillation and the two raw material streams are fed to the homogeneous plug-flow reactor resulting in a large excess of component B in this unit. In all configurations, the reaction section consists of a homogeneous PFR that is in some cases connected to a countercurrent reactive extractor, in which the reacting mixture is contacted with a fraction of the regenerated solvent.

Comparison with Conventional Designs. The Williams-Otto process designs proposed in the literature mainly follow the flowscheme shown in Figure 7 with a plug-flow or a well-mixed reactor. Balakrishna and Biegler (1993) reported on

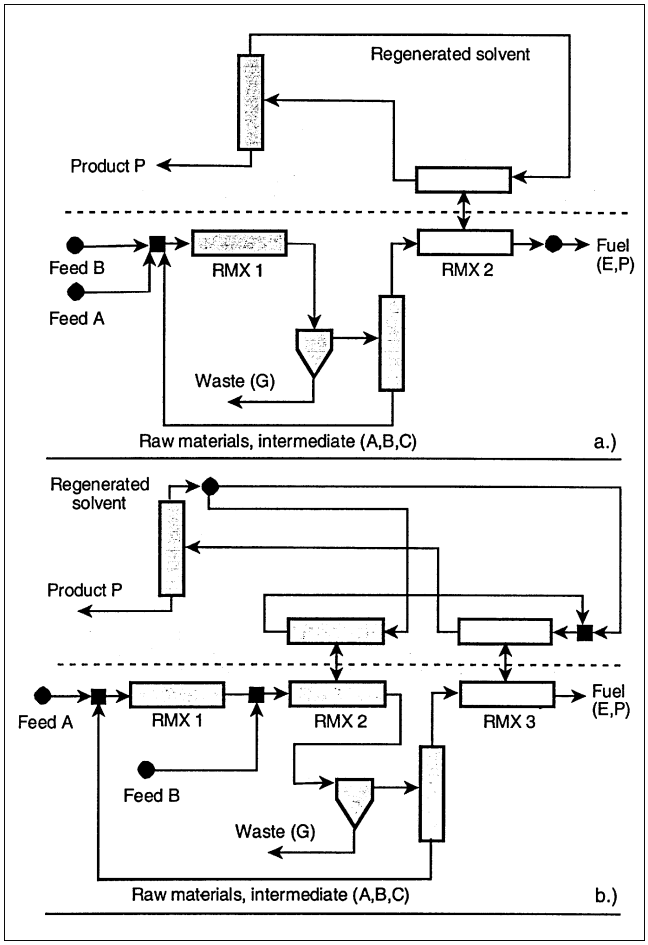

Figure 9. Reactor-hybrid separation processes from the design stage.

performance improvements of designs featuring a number of PFR stages with multiple intermediate separation $G/A,B,C,P,E$ and $P,E/A,B,C$ in the case of low separation costs. According to the cost models employed in the present study, the conventional process yields a profit of 51.5 k$/yr with a plug-flow reactor, whereas the use of a well-mixed reactor results in a slight loss (-0.7 k$/yr). Intermediate separation tasks inside the reactor network were not observed to lead improved performances as compared to the conventional designs. The novel designs featuring reactive extraction and reactor-hybrid separation arrangements exhibit significantly improved performances as compared to the conventional process configurations.

Example 2: production of ethylene glycol

The proposed synthesis framework is applied to synthesize process designs for ethylene glycol ($C_2H_6O_2$) production from ethylene oxide and water. The valuable product ethylene glycol reacts further to the unwanted byproduct diethylene glycol. The model consists of two reactions as follows

$$C_2H_4O + H_2O \rightarrow C_2H_6O_2$$
$$C_2H_4O + C_2H_6O_2 \rightarrow C_4H_{10}O_3$$

Table 3. Problem Data for the Ethylene Glycol Production Process

Reaction	Kinetics [mol/cm^3·s]	ΔH [kJ/mol]	
EO + W → EG	$3.15\times10^9 \exp[-9547/T(K)]\cdot x_{EO}\cdot x_W$	−80.0	
EO + EG → DEG	$6.30\times10^9 \exp[-9547/T(K)]\cdot x_{EO}\cdot x_{EG}$	−13.1	
Component	Vapor pressure [atm]		
EO	$71.9\cdot\exp[5.72(T(K)-469)/(T(K)-35.9)]$		
W	$221.2\cdot\exp[6.31(T(K)-647)/(T(K)-52.9)]$		
EG	$77.0\cdot\exp[9.94(T(K)-645)/(T(K)-71.4)]$		
DEG	$47.0\cdot\exp[10.42(T(K)-681)/(T(K)-80.6)]$		
Parameter	Symbol	Units	Value
Cost of Ethylene Oxide	c^{EO}	\$/kmol	43.7
Cost of water	c^W	\$/kmol	21.9
Onstream time	OP	10^3 h/yr	8.15
Hot utility cost	c^H	\$k/kW·yr	146.8×10^{-3}
Cold utility cost	c^C	\$k/kW·yr	24.5×10^{-3}

Table 3 summarizes the problem data employed in the synthesis study. In view of the highly exothermic reactions, Ciric and Gu (1994) proposed to carry out the process in a reactive distillation column. The synthesis problem was formulated as an MINLP with the feed location and the existence of trays being the binary decision variables. A reactive distillation column with distributed ethylene oxide feed was found to perform better than a two-feed reactive distillation column. Papalexandri and Pistikopoulos (1996) formulated superstructures of their multipurpose mass/heat-transfer modules for this process as MINLPs and solved for minimum utility cost. A reactive distillation column was presented as the optimal structure, and, although the superstructures include a variety of novel structures, alternative designs are not identified. In a further study, Stein et al. (1999) synthesized a reactor network of two-phase reactor-condenser elements for minimum utility cost. In agreement with the above studies, the reactive distillation column arrangement was found to perform best. By penalizing the streams of the column arrangement, Stein et al. (1999) were able to obtain novel process designs; however, the performance of the alternative design reported is significantly inferior to that of the reactive distillation column.

The process goal is the production of 25 kmol/h of ethylene glycol with a minimum purity of 95 mol. %. Ideal vapor and liquid phases are assumed (Ciric and Gu, 1994). The objective function considers raw material and utility costs as follows

$$J(k\$/yr) = OP\left(c^{EO}(FD^{EO} - FP^{EG}) + c^W(FD^W - FP^{EG})\right) + c^H H^{UT} + c^C C^{UT}$$

where FD^{EO} (kmol/h) and FD^W (kmol/h) are the feeds of ethylene oxide and water and H^{UT} (kW) and C^{UT} (kW) are the heating and cooling requirements, respectively. FP^{EG} denotes the ethylene glycol production rate and c^{EO}, c^W, c^H, c^C are cost parameters. Capital costs and treatment costs for water in the product stream are not considered here as they amount for less than 1% of the total annualized costs, as reported by Ciric and Gu (1994), and do not have a significant effect on the performance targets. The mass-transfer rates are calculated according to the film theory with driving forces calculated on a mole fraction basis. The reaction rates are set to zero inside the RMX units to realize mass exchange sections. High specific mass-transfer coefficients have been selected ($k_l a = 100$ kmol/L-h for all components) to approach the vapor-liquid equilibrium in each well-mixed cell. The optimal design of Ciric and Gu (1994) has been simulated to investigate the effect of the modeling differences on the performance of the column. Each of the six reactive stages has been represented by a reactive RMX unit with well-mixed compartments in both phases, and the four nonreactive stages are represented by a countercurrent RMX unit

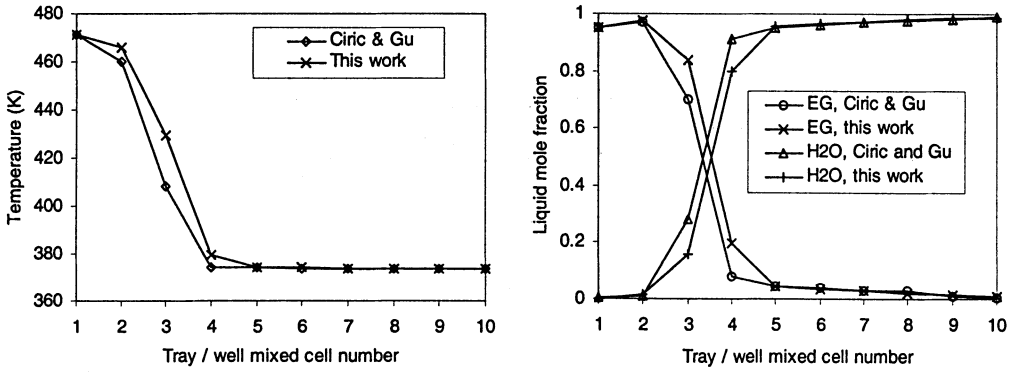

Figure 10. Model comparison for the best reactive distillation column design reported in Ciric and Gu (1994).

Table 4. Simulation of the Reactive Distillation Column of Ciric and Gu (1994)*

Tray/Well-Mixed Cell*	EO Feed (kmol/h)	H_2O Feed (kmol/h)	Reaction V_R (L)
6	4.89	0.00	551
5	4.76	0.00	482
4	4.69	0.00	448
3	4.97	0.00	371
2	0.20	0.00	1,467
1	8.05	26.31	12
Product Molar Flows (kmol/h)			
	EG	DEG	H_2O
Ciric and Gu (1994)	25.00	1.27	0.04
This work	24.98	1.29	0.04

*Boilup ratio: 0.958, trays counted from top to bottom, holdup of cells 1 through 4: 250 L.

with four well-mixed cells in each compartment. Both raw material streams are fed into the liquid phase for comparison purposes only. Table 4 presents the performance of the column structure. The rate-based model slightly produces a deteriorated selectivity towards ethylene glycol. Figure 10 shows the temperature and composition profiles of the column for both models. In the reaction section, the profiles obtained from both models are virtually identical. The mass-transfer effects lead to slight variations in the mass exchange section, where the ethylene glycol fractions and temperatures are found to be higher and the water mole fractions lower, as compared to the equilibrium stage model. The optimal column of Ciric and Gu (1994) is infeasible, as it does not meet the ethylene glycol production constraint when simulated using the rate-based model. The evaluation of the objective function reveals a performance of \$2,336/yr for the column.

Network superstructures are postulated accounting for vapor and liquid phases. A maximum of four multiphase RMX units are allowed (up to five well-mixed cells in each compartment). The stream network includes complete intraphase as well as interphase connectivity among all compartments of the generic units present. Network optimization reveals a performance target of around \$2,180 k/yr for the system, an improvement of 7% over the optimal reactive distillation column. A number of designs exist that exhibit performances close to the target. Figure 11 shows two design alternatives of similar performance. The design data are summarized in Table 5.

All designs obtained from the search feature four active RMX units with five well-mixed cells in each of the compartments. Reaction takes place in three of the units whereas one is observed to be a mass exchanger. Common to all designs is a countercurrent mass exchanger with a liquid to vapor interphase recycle (reboiler) in which the water and ethylene oxide are stripped off the glycol mixture leaving the reaction zone. Significant differences are observed with respect to the design of the reaction network. In terms of contacting patterns, design alternatives with only countercurrent (Figure 11a) and with only cocurrent RMX units exist (Figure 11b). Combinations of co- and countercurrent units are also observed. A serial arrangement of the liquid-phase compartments is facilitated in most designs. The reaction volumes utilized in the different flow schemes vary significantly from

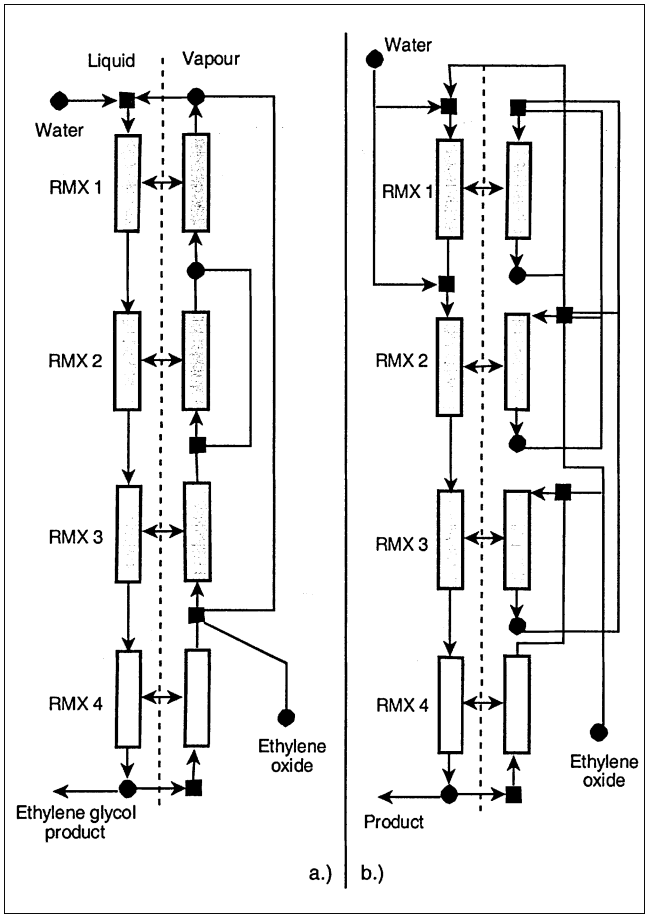

Figure 11. Design alternatives with purely countercurrent and cocurrent reaction zones (gray units indicate reactive RMX units).

around 100 L to beyond 3,000 L. The water is generally fed to the first two RMX units, whereas the ethylene oxide is distributed among the last two reactive units. Intraphase vapor recycles around combinations of reactive units are observed in all designs. Ciric and Gu (1994) have constrained the vapor flow inside the column to a maximum of 1,000 kmol/h, a value found to be conservative by Cardoso et al. (2000). Although not imposed in this work, the maximum

Table 5. Design Information for Process Configurations of Figure 11

		Fig. 11a	Fig. 11b
Objective	\$k/yr	2,181	2,252
Feed ethylene oxide	kmol/h	27.56	27.56
Feed water	kmol/h	26.30	26.30
Product purity	Mol. %	95.06	95.06
Reaction volume (RMX 1)	L	398	35
Reaction volume (RMX 2)	L	154	845
Reaction volume (RMX 3)	L	89	699
Total reaction volume	L	641	1,579
Heating duty	MW	5.93	6.34
Cooling duty	MW	6.82	7.23
Maximum vapor flow	kmol/h	819	4,301

vapor flow in most designs obtained in this study are well below the upper bound of Ciric and Gu (1994). In some designs, vapor flows as high as 4,300 kmol/h are observed; however, they offer similar, but not superior, performance and can thus be ignored if these high vapor flows are found to be impractical in more detailed simulation studies.

The novel designs compare favorably with the reactive distillation columns presented in earlier studies, as a result of reduced energy requirements. Stein et al. (1999) and Ciric and Gu (1994) report a heating duty of 6.7 MW for the optimal reactive distillation column. It is anticipated that this reduction is a result of the local vapor recycle policies. As compared to the reactive distillation column, higher vapor flows are realized in the reacting sections in order to maintain a consistently low ethylene oxide concentration in the liquid phase, whereas the stripping section is operated at lower vapor flows. The water to ethylene oxide ratio is greater than 600/1 throughout the reacting sections of all designs obtained. For comparison, the lowest water to ethylene oxide ratio in the optimal column of Ciric and Gu (1994) is reported to be 200/1 (a ratio of 204/1 is obtained from the rate-based model). Figure 12 shows the mole fraction and temperature profiles along the reaction volume of the design shown in Figure 11a. Cardoso et al. (2000) report improved reactive distillations designs with up to three times higher heating and cooling requirements as compared to the design of Ciric and Gu (1994). Such designs have not been observed in this work and the savings reported here stem from reductions in energy requirements; indeed, the reported optimal designs of Cardoso et al. (2000) have performances of \$2,600 k/yr and \$3,872 k/yr for the objective function considered in this work.

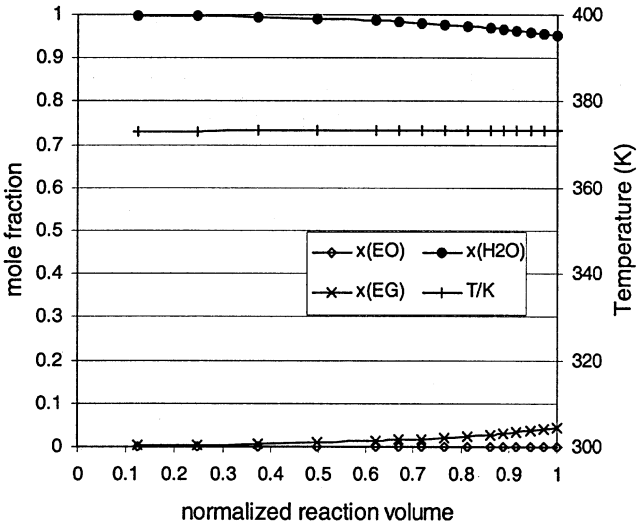

Figure 12. Mole fraction and temperature profiles along the reaction zones (design of Figure 8a).

Example 3: activated sludge processes

The proposed synthesis methodology is applied to establish performance targets and design guides for activated sludge processes. The process behavior is predicted using the Activated Sludge model No. 1 developed by Henze et al. (1987), which has been verified under a variety of operating conditions (Dold and Marais, 1986) and has subsequently been the base of a range of commercial and educational simulation software developments. The reaction processes involve two main reaction paths

Carbonaceous Organics Reaction Path

$$X_S \xrightarrow{O_2, NO, X_{BH}} S_S$$

$$S_S + O_2 \xrightarrow{X_{BH}} X_{BH}$$

$$S_S + NO_3^- \xrightarrow{X_{BH}} X_{BH} + N_2$$

Table 6. Rate Expressions of the Model (Henze et al., 1987)

Process	Process Rate ($M \cdot L^{-3} \cdot T^{-1}$)
Aerobic growth of heterotrophs	$\mu_H \left(\frac{S_S}{K_S + S_S} \right) \left(\frac{S_O}{K_{O,H} + S_O} \right) X_{BH}$
Anoxic growth of heterotrophs	$\mu_H \left(\frac{S_S}{K_S + S_S} \right) \left(\frac{K_{O,H}}{K_{O,H} + S_O} \right) \left(\frac{S_{NO}}{K_{NO} + S_{NO}} \right) n_g X_{BH}$
Aerobic growth of autotrophs	$\mu_A \left(\frac{S_{NH}}{K_{NH} + S_{NH}} \right) \left(\frac{S_O}{K_{O,A} + S_O} \right) X_{BA}$
Decay of heterotrophs	$b_h X_{BH}$
Decay of autotrophs	$b_A X_{BA}$
Ammonification of soluble organic nitrogen	$k_h S_{ND} X_{BH}$
Hydrolysis of entrapped organics	$k_h \frac{\frac{X_S}{X_{BH}}}{K_X + \frac{X_S}{X_{BH}}} \cdot \left[\left(\frac{S_{O,H}}{K_{O,H} + S_O} \right) + n_h \left(\frac{S_S}{K_S + S_S} \right) \left(\frac{S_{NO}}{K_{NO} + S_{NO}} \right) \right] X_{BH}$
Hydrolysis of entrapped organic nitrogen	$k_h \frac{\frac{X_S}{X_{BH}}}{K_X + \frac{X_S}{X_{BH}}} \cdot \left[\left(\frac{S_{O,H}}{K_{O,H} + S_O} \right) + n_h \left(\frac{S_S}{K_S + S_S} \right) \left(\frac{S_{NO}}{K_{NO} + S_{NO}} \right) \right] X_{BH} \cdot \frac{X_{ND}}{X_S}$

Table 7. Wastewater Composition (Henze et al., 1987)

Constit.	Unit	Content	Constit.	Unit	Content
S_S	g COD m^{-3}	30	X_{ND}	g N·m^{-3}	7.2
S_I	g COD m^{-3}	30	S_{NH}	g NH_3– N·m^{-3}	16
X_S	g COD m^{-3}	125	S_{NO}	g NO_3– N·m^{-3}	0
X_I	g COD m^{-3}	25	X_{AUT}	g COD m^{-3}	1
S_{ND}	g N·m^{-3}	1.2	X_{HET}	g COD m^{-3}	30

Organic Nitrogen Reaction Path

$$X_{ND} \xrightarrow{O_2, NO, X_{BH}} S_{ND}$$

$$S_{ND} \xrightarrow{X_{BH}} S_{NH}$$

$$S_{NH} + O_2 \xrightarrow{X_{BA}} X_{BA} + NO_3^-$$

$$S_S + NO_3^- \xrightarrow{X_{BH}} X_{BH} + N_2$$

where X denotes particulate material and S denotes soluble material. The highly nonlinear reaction kinetics are given in Table 6. A water feed flow rate of 100 m^3/h is considered. The wastewater composition and the model parameters are summarized in Tables 7 and 8. The gas-liquid equilibrium was calculated using the Henry's constants reported in Metcalf and Eddy (1991).

Superstructures featuring three reactive RMX units and a single separation task unit for the separation of the purified water that form the sludge were subjected to optimization. It was assumed that the sludge separator achieves only a nonsharp split with the water equally distributing among the outlet streams. The mass-transfer switches allow to facilitate the oxic and anoxic reaction sections of interest. As the process needs to simultaneously remove nitrogen, as well as organic matter, the performance index employed in this work gives a weighted account of the chemical oxygen demand (COD) and the total amount nitrogen containing fractions (N) that are present in the effluent stream

$$J = 100\left(\frac{COD}{COD_0} + \frac{N}{N_0}\right)$$

As the amount of treated water is not accounted for in the objective function, there is a constraint on the amount of sludge that can be purged from the process. It was found that the whole sludge, and with it a significant amount of water, is wasted in the unconstrained optimal designs. The water loss with the sludge is constraint to amount for less than 5 m^3/h.

The target performance of the activated sludge system for simultaneous removal of nitrogen and organic matter has been located at an objective value of around 270. A design that achieves a performance of 267 is shown in Figure 13a. The process has reduced the COD by 96.8% and the total nitrogen content by 84.8%. Process structures generally feature plug-flow compartments in the gas and liquid phases. Both, co- and countercurrent phase contacting is observed. The designs feature oxic and anoxic sections with the latter having the largest volume requirements. In the oxic reaction sections, the oxygen concentrations are approaching the equi-

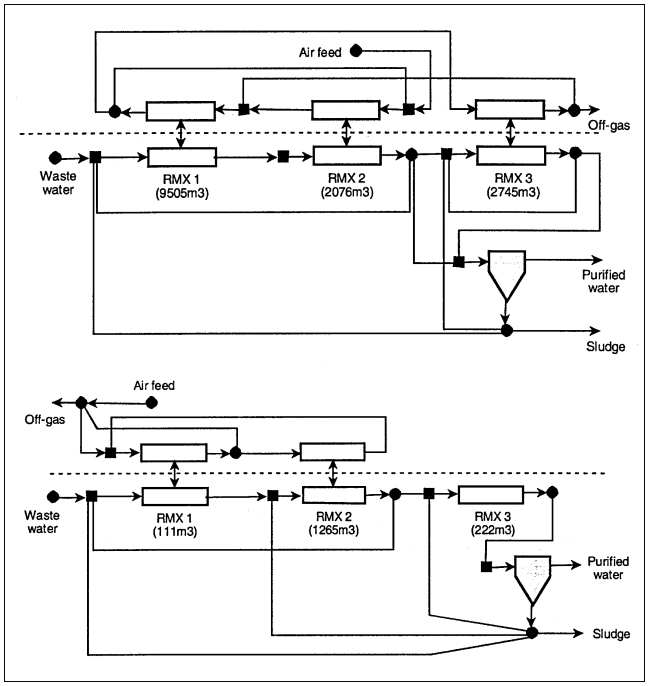

Figure 13. Volume unconstrained and constrained designs achieving the performance target of the activated sludge process.

Table 8. Model Parameters (Henze et al., 1987)

Description	Symbol	Unit	Value
Heterotrophic yield	Y_H	–	0.67
Autotrophic yield	Y_A	–	0.24
Fraction of biomass yielding particulate products	f_p	–	0.08
Mass N/Mass COD in biomass	i_{XB}	g N(g COD)$^{-1}$	0.086
Mass N/Mass COD in biomass products	i_{XP}	g N(g COD)$^{-1}$	0.06
Maximum specific growth rate for heterotrophs	μ_H	d^{-1}	6
Substrate half-saturation coefficient	K_s	g COD m^{-3}	20
Oxygen half-saturation coefficient for autotrophs	$K_{O,H}$	g/m^3	0.2
Nitrate half-saturation coefficient for heterotrophs	K_{NO}	g NO_3-N·m^{-3}	0.5
Decay coefficient for heterotrophic biomass	b_H	d^{-1}	0.62
Maximum specific growth rate for autotrophs	μ_A	d^{-1}	0.8
Oxygen half-saturation coefficient for autotrophs	$K_{O,A}$	g O_2·m^{-3}	0.4
Ammonia half-saturation coefficient	K_{NH}	g NH_3-N·m^{-3}	1
Decay coefficient for autotrophic biomass	b_A	d^{-1}	
Correction factor for anoxic growth	n_g	–	0.8
Ammonification	k_a	m^3cod^{-1}·d^{-1}	0.08
Maximum specific hydrolysis rate	k_h	d^{-1}	3
Half-saturation coefficient for hydrolysis	K_x	–	0.03
Correction factor for anoxic hydrolysis	n_h	–	0.4

librium concentrations that can be achieved by contacting air with water. The designs facilitate wastewater and air recycles among the individual RMX units. Concentrated sludge is distributed among the individual RMX units. Generally, the designs obtained require fairly large reactor volumes (around 16,000 m^3), which is certainly undesired from a practical, as well as from an economical, viewpoint.

In a subsequent study, an upper network volume bound of 1,600 m^3 has been introduced for the RMX units, corresponding to a reduction by one order of magnitude as compared to the volumes observed previously. Again, the target performance of the activated sludge system has been located at an objective value of around 270. A design that achieves a performance of 271 is shown in Figure 13b. Despite the reduced network volume, the process has reduced the COD by 97.5% and the total nitrogen content by 84.9%. All designs obtained from the stochastic optimization closely approach the upper volume bound. As previously, the process structures generally feature plug-flow compartments in the gas and liquid phases with co- as well as countercurrent phase contacting.

Despite the similar design structures observed for the two cases studied, a closer inspection reveals a rather different processing strategy. Figure 14 shows the oxygen concentrations in the liquid-phase well-mixed cells in the individual RMX units. It can be seen that the volume-unconstraint design has distinct oxic and anoxic sections. The oxygen concentrations approach zero in the liquid phase of the anoxic RMX units, whereas high concentrations between 3 and 7 ppm are found in the oxic sections. In the volume-constraint design on the other hand, intermediate oxygen concentrations of around 0.2 ppm are observed in the oxic sections. This suggests that both the total nitrogen and the organic matter has degraded in the oxic reactor. In all conventional activated sludge process designs, the oxic and anoxic reaction sections are strictly separated with the former sections being operated at oxygen concentrations, as high as achievable to maximize the rate of COD reduction. This is an outcome of the insights into activated sludge processes that the different reactions occur under different conditions with respect to oxygen presence, as they trigger different kinds of microbial metabolisms. The rates of COD and total nitrogen reduction are maximized by high oxygen concentrations and in the absence of oxygen, respectively. Optimal designs, however, seem to be operated at very low oxygen concentrations and thus allow for only slow rates of COD reduction, but simultaneously enable the removal of nitrogen.

The validity of the observations made in this study depends upon the validity of the Activated Sludge model No. 1 in the low oxygen concentration region. It should be noted that the model has been developed for the simulation of existing processes, that is, those with a clear separation of oxic and anoxic reaction sections. To allow different kinetics to be switched on and off depending upon whether oxygen is present, the model facilitates several Monod-type terms that activate or deactivate the appropriate kinetic expressions. These terms are not a result of mechanistic insights (this does not imply that they represent wrong trends), but rather functions that allow the activation and deactivation of the reactions in the different regimes without introducing discontinuities into the model equations. The oxygen-related term of the form S/(K + S) is employed to activate aerobic processes (S: oxygen concentration, K constant), that is, it approaches zero and unity at high and low oxygen concentrations, respectively. The optimal designs facilitate oxygen concentrations such that the oxygen concentration is of the same order of magnitude as constants K. Also, the Monod-type terms do not activate or deactivate any reactions, but rather allow all reactions to occur simultaneously at reduced rates. A thorough study of the activated sludge process regarding different wastewater compositions, pure oxygen feeds and different kinetic parameters has been performed using the optimization technology proposed in this work (Rigopoulos and Linke, 2002).

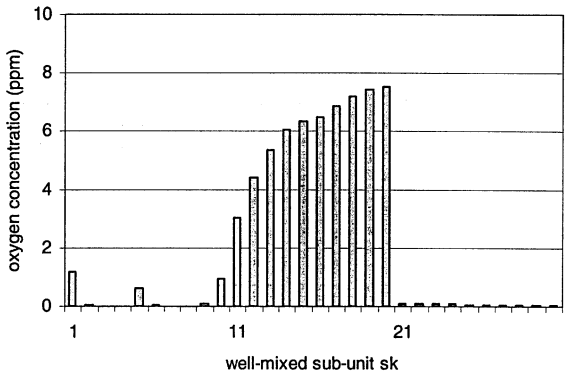

a. Oxygen concentration in the liquid phase of design shown in Fig. 13a.

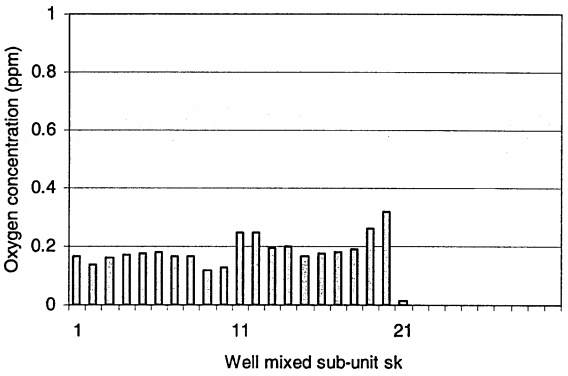

b. Oxygen concentration in the liquid phase of design shown in Fig. 13b.

Figure 14. Oxygen concentration in the liquid phase of activated sludge processes.

RMX1: $sk \in [1, 10]$, RMX2: $sk \in [11, 20]$, RMX3: $sk \in [21, 30]$, sk: well-mixed cell.

Example 4: hybrid separations for natural gas sweetening

To illustrate the possibilities for the proposed synthesis framework to take up applications in separation system design, we synthesize optimal hybrid adsorption/membrane process configurations for the sweetening of crude natural gas to meet the pipeline specifications ($CO_2 < 2$ vol. %, $H_2S < 4$ ppm). Superstructures featuring two states (high and low pressure), three RMX units and three STUs in the high-pressure state are generated and subjected to optimization. The RMX units represent the membrane modules, whereas

Table 9. Problem Data for the Gas Sweetening Case Study

Gas Permeabilities (P/δ)		
Methane (CH_4)	m/bar-s	7.50×10^{-6}
Nitrogen (N_2)	m/bar-s	7.50×10^{-6}
Carbon dioxide (CO_2)	m/bar-s	1.65×10^{-4}
Hydrogen sulfide (H_2S)	m/bar-s	7.65×10^{-4}
Feed flow rate	m^3/s	10
Feed pressure	bar	45
Retentate pressure	bar	>1.5
Feed Composition		
Methane (CH_4)	Mol.%	79
Nitrogen (N_2)	Mol.%	1
Acid gases	Mol.%	20
Capital Costs		
Membrane module	$\$/m^2$	$100\ A^{0.6}$
Compressor	\$	$6{,}000\ HP^{0.7}$
Compr. efficiency	%	70
Plant life	yrs	10
Membrane cost	$\$/m^2$	60
Operating Costs		
Power	\$/kWh	0.03
Membrane life span	yrs	3
Methane losses	\$/GJ	2
Onstream time	h/yr	8,500

the irreversible adsorption process is represented by the separation task units. The stream network facilitates intraphase streams in both states, as well as interstate streams from sources originating in the low-pressure state, which are associated with compressors. The properties of the employed poly(ether urethane urea) membranes (Chatterjee et al., 1997) are summarized in Table 9, along with the feed conditions and pressures. A total of 15 well-mixed units are utilized to approximate the plug-flow behavior in the RMX compartments. The fixed-bed adsorption process considered allows to selectively remove the hydrogen sulfide below the level of detection (Carnell et al., 1995) and is modeled as a separation task which performs a sharp split between the H_2S and the remaining components present in the inlet stream. The pressures within the compartments of both states are not considered as degrees of freedom for sake of simplicity; however, an additional move to facilitate this can easily be introduced into the optimization framework. The objective function employed in the synthesis study is the total annualized cost of the process, which is to be minimized. All cost data employed in the synthesis study are summarized in Table 9. Additionally, the cost of the fixed-bed adsorption process is assumed to be \$50/kg of hydrogen sulfide adsorbed, which includes the pressure vessel as well as the regeneration and recycling of the adsorbent. Two feed compositions are considered, each containing a total of 20 mol. % of acid gases (H_2S, CO_2). Feed 1 contains 1 mol. % of H_2S and Feed 2 contains 4 mol. % of H_2S.

Figure 15 shows optimal process configurations obtained for the two feedstreams. The corresponding design information is summarized in Table 10. All membrane modules observed in the structures feature plug-flow compartments in both states with countercurrent stream contacting. Figure 15a shows an arrangement for a feed concentration of $C_{H2S} = 1$ vol. %. The feed gas is fed to the first membrane module, the retentate of which contributes to the flow into the second

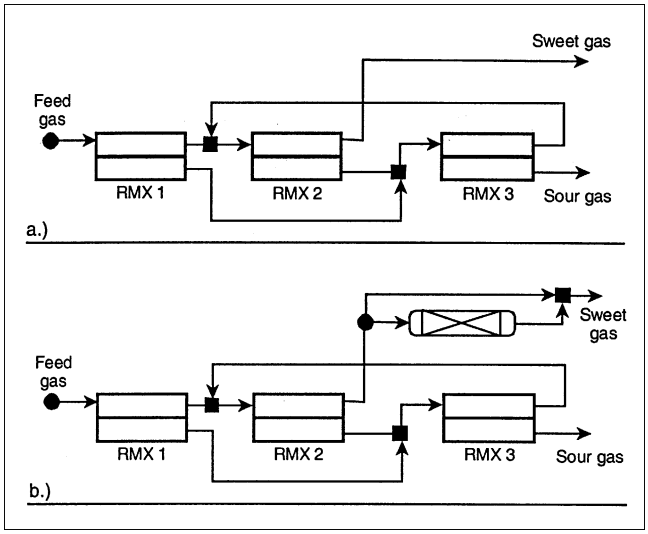

Figure 15. Close-to-target process configurations for gas sweetening.

(a) $C_{H_2S} = 1$ vol. %; (b) $C_{H_2S} = 4$ vol. %.

module. Both permeate streams of the first and second module are compressed and fed to a third membrane unit. The retentate of this unit is recycled to the second module. The sweet gas product stream is obtained as the permeate stream of the second module. For Feed 2, the process configurations (Figure 15b) exhibit a similar topology in terms of membrane module arrangements. A fraction of the sweetened effluent of the membrane network is fed to an irreversible adsorption process where the hydrogen sulfide is completely removed before the gas is fed to the final sweet gas product. The remainder of the membrane network effluent is bypassed directly to the final sweet gas product such that the pipeline specification is closely met.

Computational Demands

All results presented in this article have been obtained on a SUN Enterprise HPC 4500 workstation computer with eight 400 MHz UltraSPARC-II processors each with 8 MB external cache. The CPU times are comparable to those observed on a Pentium PIII 600 Mhz personal computer in a comparative study.

The key parameter characterizing the thoroughness of the optimal search using SA is the Markov chain length (MC). Small chains generally correspond to premature convergence of stochastic experiments. In order to ensure good conver-

Table 10. Process Data of Hybrid Separation Designs of Figures 19 and 20

H_2S Content in Feed	1 vol. %	4 vol. %
Objective (\$k/yr)	914	967
RMX 1 (m^2)	157	1,544
RMX 2 (m^2)	4,871	3,837
RMX 3 (m^2)	518	493
Total area (m^2)	5,546	5,874
Methane loss (kmol/s)	0.09	0.09
H_2S adsorbed (kg/yr)	—	1,816

gence, the synthesis studies are performed for a set of optimization runs starting from short Markov chain length (MC = 6) and subsequently increased until all runs converge to within a prescribed confidence region around the target objective (best performance found). Thus, all results reported in this article have converged in a stochastic sense. The Markov chain length (MC) has been increased until the standard deviation of the objectives from the optimal solutions of a set of twelve stochastic experiments has fallen below 5%, except for the activated sludge process. The computational burden posed by the stochastic search depends upon the demanded confidence levels, as well as the nature of the simulation problem. The average optimization performances for the individual problems are summarized in Table 11.

As expected, the simplest synthesis problem, the gas sweetening study, requires the least search time to achieve good convergence. The simulations of the individual structures are extremely fast so that the search of an average of more than 3,000 states can be completed in under 10 min of CPU time. As more complexity is added to the synthesis problem, the computational demand increases as

(a) a result of mainly an increase in the time required to evaluate the individual states (ethylene glycol production process, Activated Sludge process) and/or

(b) an increase in the combinatorial problem size (Williams-Otto process).

Clearly, the most challenging optimization problem addressed in this work is the activated sludge process synthesis. The highly nonlinear process models and the large number of components incur a mere 6 s for a single state evaluation and the average runs converge after 15 to 25 h. This appears excessive for an optimization study; however, in view of the years of various researchers' time that has been spent on this highly complex design problem, this amount of time appears rather small. The chance of identifying high-quality designs within a couple of days of an engineer's time should encourage the active use of the proposed synthesis scheme. At the same time, there is a future research challenge to fasten up the synthesis technology.

Concluding Remarks

A new framework for the synthesis of chemical processes involving reaction and separation is presented. The methodology utilizes superstructures that are generated from combinations of generic synthesis units to capture the possible processing alternatives and provide a venue for optimization. The system representation is not constrained to conventional reactor-separator or reactive separation designs, but instead accounts for any novel combination of the synthesis units and their functionalities. Stochastic optimization techniques in the form of simulated annealing are used to determine the performance targets and a set of optimal designs from the superstructure. A major advantage of the synthesis technology is its ability to determine performance targets and to identify a variety of design options with similar close-to-target performances that allow the design engineer to inspect similarities and differences in order to develop an understanding of the optimal design patterns.

The proposed developments have been illustrated with a number of case studies to demonstrate the results that can be expected from such an approach and the wide range of possible applications, including reactive separation, reactive-reaction/separation, and hybrid separation systems. As has become apparent from these case studies, the stochastic optimization algorithms offer a major advantage as the searches provide multiple optimal designs. Unconventional, novel designs have been obtained for all the examples presented.

The approach facilitates a simulator to solve the balance equations of the design instances which the stochastic search procedure selects from the superstructure. It is possible to interface the simulator employed in the proposed methodology with detailed process models and quickly generate the superstructure models for problems of any size and complexity. In doing so, one should bear in mind that the computational demand of the procedure strongly depends upon the size of the simulation problem (the number of species and synthesis units considered) and its complexity in terms of the nonlinearities and discontinuities of the problem specific models (physical property models, phase equilibrium calculations, mass-transfer rates, and reaction kinetics). The purpose of the proposed approach lies in conceptual design. The approach is intended for use in rapid screening of vast numbers of possible design alternatives to extract those few promising ones that should be studied in greater detail in subsequent stages. In order to prevent prohibitive CPU times, it is advisable to refrain, whenever possible, from adding unnecessary modeling detail to the formulation that does not affect the *conceptual* design insights that can be gained for the system at hand. This is not always possible and future research challenges are therefore:

- The development of systematic techniques for process model size and complexity reduction, in particular for reaction kinetics; and
- The development of systematic design pre-screening approaches using *a priori* analysis of modeling knowledge to reduce the search space and to "lead" the optimization. Ongoing research focuses on the development of such approaches based on data mining techniques and will be the subject of future publications.

Table 11. Computational Information on the Case Studies

Case Study	Std. Dev. (%)	Markov Chain Length	States Evaluated	Spec. CPU Time* (s)
Williams-Otto process	4.1	60	11,136	0.5
Ethylene glycol production	2.6	40	9,547	3.2
Activated sludge process	12	40	13,259	6.2
Gas sweetening	0.9	60	8,075	0.7

*Average CPU time for a single state evaluation.

Acknowledgments

The main part of the work has been carried out at the Dept. of Process Integration at UMIST (University of Manchester Institute of Science and Technology). The authors wish to express their gratitude to the UMIST Process Integration Research Consortium for providing the research funding.

Literature Cited

Aarts, E. H. L., and P. G. M. van Laarhoven, "Statistical Cooling: A General Approach to Combinatorial Optimization Problems," *Philips J. Res.*, **40**, 193 (1985).

Balakrishna, S., and L. T. Biegler, "A Unified Approach for the Simultaneous Synthesis of Reaction, Energy, and Separation Systems," *Ind. Eng. Chem. Res.*, **32**, 1372 (1993).

Barbosa, D., and M. F. Doherty, "The Simple Distillation of Homogeneous Reactive Mixtures," *Chem. Eng. Sci.*, **43**, 541 (1988).

Cardoso, R. L. Salcedo, S. Feyo de Azevedo, and D. Barbosa, "Optimization of Reactive Distillation Processes with Simulated Annealing," *Chem. Eng. Sci.*, **55**, 5059 (2000).

Carnell, P. J. H., K. W. Joslin, and P. R. Woodham, "Fixed-Bed Processes Provide Flexibility for COS, H_2S Removal," *Oil Gas J.*, **52**, 93 (1995).

Chatterjee, G., A. A. Houde, and S. A. Stern, "Poly(ether urethane) and Poly(ether urethane urea) Membranes with High H_2S/CH_4 Selectivity," *J. Mem. Sci.*, **135**, 99 (1997).

Ciric, A. R., and D. Gu, "Synthesis of Nonequilibrium Reactive Distillation Processes by MINLP Optimization," *AIChE J.*, **40**, 1479 (1994).

Dold, P. L., and G. v. R. Marais, "Evaluation of the General Activated Sludge Model Proposed by the IAWPRC Task Group," *Wat. Sci. Tech.*, **18**, 63 (1986).

Fraga, E. S., "The Automated Synthesis of Complex Reaction/Separation Processes using Dynamic Programming," *Chem. Eng. Res. Des.*, **74**, 249 (1996).

Hauan, S., A. W. Westerberg, and K. M. Lien, "Phenomena-Based Analysis of Fixed Points in Reactive Separation Systems," *Chem. Eng. Sci.*, **55**, 1053 (2000a).

Hauan, S., A. R. Ciric, A. W. Westerberg, and K. M. Lien, "Difference Points in Extractive and Reactive Cascades. I—Basic Properties and Analysis," *Chem. Eng. Sci.*, **55**, 3145 (2000b).

Henze, M., C. P. L. Grady Jr., W. Gujer, G. v. R. Marais, and T. Matsuo, "Activated Sludge Model No.1," *IAWPRC Scientific and Technical Reports No. 1*, IAWPRC, London (1987).

Ismail, R. S., E. N. Pistikopoulos, and K. P. Papalexandri, "Modular Synthesis Framework for Combined Separation/Reaction Systems," *AIChE J.*, **47**, 629 (2001).

Ismail, R. S., E. N. Pistikopoulos, and K. P. Papalexandri, "Synthesis of Combined Reactive and Reactor/Separation Systems Utilizing a Mass/Heat Exchange Transfer Module," *Chem. Eng. Sci.*, **54**, 2721 (1999a).

Ismail, R. S., E. N. Pistikopoulos, and K. P. Papalexandri, "Modular Representation Synthesis Framework for Homogeneous Azeotropic Separation," *AIChE J.*, **45**, 1701 (1999b).

Kirkpatrick, S., C. D. Gelatt, and M. P. Vecchi, "Optimization by Simulated Annealing," *Science*, **220**, 671 (1983).

Kokossis, A. C., and C. A. Floudas, "Synthesis of Isothermal Reactor-Separator-Recycle Systems," *Chem. Eng. Sci.*, **46**, 1361 (1991).

Lakshmanan, L., and L. T. Biegler, "Synthesis of Optimal Chemical Reactor Networks with Simultaneous Mass Integration," *Ind. Eng. Chem. Res.*, **35**, 4523 (1996).

Marcoulaki, E. C., and A. C. Kokossis, "Screening and Scoping Complex Reaction Networks Using Stochastic Optimization," *AIChE J.*, **45**, 1977 (1999).

Mehta, V. L., and A. C. Kokossis, "Nonisothermal Synthesis of Homogeneous and Multiphase Reactor Networks," *AIChE J.*, **46**, 2256 (2000).

Mehta, V. L., and A. C. Kokossis, "Development of Novel Multiphase Reactors using a Systematic Design Framework," *Comp. Chem. Eng.*, **21**, S325 (1997).

Mehta, V. L., "Synthesis and Optimisation of Multiphase Reactor Networks," PhD Thesis, UMIST, U.K. (1998).

Metcalf and Eddy, *Wastewater Engineering: Treatment, Disposal, Reuse*, 3rd ed., G. Tchobanoglous and F. L. Burton, eds., McGraw Hill, New York (1991).

Metropolis, N., A. W. Rosenbluth, M. N. Rosenbluth, A. H. Teller, and E. Teller, "Equation of State Calculations for Fast Computing Machines," *J. Chem. Phys.*, **21**, 1087 (1953).

Ng, K. M., and D. A. Berry, "Synthesis of Reactive Crystallization Processes," *AIChE J.*, **43**, 1737 (1997).

Ng, K. M., and K. D. Samant, "Synthesis of Extractive Reaction Processes," *AIChE J.*, **44**, 1363 (1998).

Nisoli, A., M. F. Malone, and M. F. Doherty, "Attainable Regions for Reaction with Separation," *AIChE J.*, **44**, 1363 (1997).

Okasinski, M., and M. F. Doherty, "Design Methods for Kinetically Controlled, Staged Reactive Distillation Columns," *Ind. Eng. Chem. Res.*, **37**, 2821 (1998).

Papalexandri, K. P., and E. N. Pistikopoulos, "Generalized Modular Representation Framework for Process Synthesis," *AIChE J.*, **42**, 1010 (1996).

Ray, H., and J. Szekely, *Process Optimization*, Wiley, New York (1973).

Rigopoulos, S., and P. Linke, "Systematic Development of Optimal Activated Sludge Process Designs," *Comp. Chem. Eng.*, **26**, 585 (2002).

Shah, P. B., and A. C. Kokossis, "New Synthesis Framework for the Optimization of Complex Distillation Systems," *AIChE J.*, **48**, 527 (2002).

Stein, E., A. Kienle, A. R. J. Esparta, K. D. Mohl, and E. D. Gilles, "Optimization of a Reactor Network for Ethylene Glycol Synthesis —An Algorithmic Approach," *Comp. Chem. Eng.*, **23**, S903 (1999).

Smith, E. M. B., and C. C. Pantelides, "Design of Reaction/Separation Networks Using Detailed Models," *Comp. Chem. Eng.*, **19**, S83 (1995).

Appendix: Superstructure Model Formulation

The first set of variables include the flow rates of the individual components through the synthesis units, splitters as well as mixers

$FD_{s,f,cp}$:	component flow rate through splitters $sp \in SP^F_{s,f}$
$INR_{s,rm,sk,cp}$:	component flow rate through mixers $mi \in MI^{RM}_{s,rm,sk}$
$INPR_{s,rm,cp}$:	component flow rate through mixers $mi \in MI^{PRM}_{s,rm}$
$OUTR_{s,rm,cp}$:	component flow rate through splitters $sp \in SP^{RM}_{s,rm}$
$OUTSK_{s,rm,sk,cp}$:	component flow rate through splitters $sp \in SP^{IRM}_{s,rm,sk}$
$INS_{s,st,cp}$:	component flow rate through mixers $mi \in MI^{ST}_{s,st}$
$OUTS_{s,st,so,cp}$:	component flow rate through splitters $sp \in SP^{ST}_{s,st,so}$
$INP_{s,p,cp}$:	component flow rate through mixers $mi \in MI^{P}_{s,p}$
$OUTP_{s,p,cp}$:	component flow rate through splitters $sp \in SP^{P}_{s,p}$

A second set of variables includes the set of split fractions of streams connecting splitters to the individual mixers of the superstructure scheme

$SFR_{s,s^*,f,rm,sk}$: fraction of $FD_{s,f,cp}$ entering mixer $mi \in MI^{RM}_{s^*,rm,sk}$

$SFS_{s,s^*,f,st}$: fraction of $FD_{s,f,cp}$ entering mixer $mi \in MI^{ST}_{s^*,st}$

$SFP_{s,s^*,f,p}$: fraction of $FD_{s,f,cp}$ entering mixer $mi \in MI^{P}_{s,p}$

$SRR_{s,s^*,r,rm,sk}$: fraction of $OUTR_{s,r,cp}$ entering mixer $mi \in MI^{RM}_{s^*,rm,sk}$

$SRS_{s,s^*,r,st}$: fraction of $OUTR_{s,r,cp}$ entering mixer $mi \in MI^{ST}_{s^*,st}$

$SRP_{s,s^*,r,p}$: fraction of $OUTR_{s,r,cp}$ entering mixer $mi \in MI^{P}_{s,p}$

$SSR_{s,s^*,sts,so,rm,sk}$: fraction of $OUTS_{s,sts,so,cp}$ entering mixer $mi \in MI^{RM}_{s^*,rm,sk}$

$SSS_{s,s^*,sts,so,st}$: fraction of $OUTS_{s,sts,so,cp}$ entering mixer $mi \in MI^{ST}_{s^*,st}$

$SSP_{s,s^*,sts,so,p}$: fraction of $OUTS_{s,sts,so,cp}$ entering mixer $mi \in MI^{P}_{s,p}$

$SPR_{s,s^*,p,rm,sk}$: fraction of $OUTP_{s,p,cp}$ entering mixer $mi \in MI^{RM}_{s^*,rm,sk}$

$SPS_{s,s^*,p,st}$: fraction of $OUTP_{s,p,cp}$ entering mixer $mi \in MI^{ST}_{s^*,st}$

$SKP_{s,rm,sk,rp}$: fraction of $OUTSK_{s,rm,sk,cp}$ entering mixer $mi \in MI^{PRM}_{s,rm}$

Variables and parameters associated with the reaction and mass-transfer rates include

$RXR_{s,rx,rm,sk}$: specific reaction rate of reaction $rx \in RX^{A}_{s,rm}$ in $sk \in SK_{s,rm}$

$V_{s,rm}$: reaction volume of $sk \in SK_{s,rm}$

$\epsilon_{s,rm,sk}$: phase holdup of state $s \in S$ in $sk \in SK_{s,rm}$

$\nu_{s,rx,cp}$: stoichiometric coefficient of component $cp \in CP_s$ in $rx \in RX^{A}_{s,rm}$

$MTR_{s^*,s,rm,sk,cp}$: rate of mass transfer from $s^* \neq s \in S$ to $sk \in SK_{s,rm}$

The mathematical model of the superstructure consists of the following balance equations

Mixers prior to RMX compartments $mi \in MI^{RM}_{s,rm,sk}$

$$\sum_{s^* \in S} \sum_{f \in F^A_{s^*}} FD_{s^*,f,cp} SFR_{s^*,s,f,rm,sk} + \sum_{s^* \in S} \sum_{r \in RM^A} OUTR_{s^*,r,cp} SRR_{s^*,s,r,rm,sk} + PREV_{sk} + \sum_{s^* \in S} \sum_{st \in ST^A_{s^*}} \sum_{so \in SO_{s^*,st}} OUTS_{s^*,st,so,cp} SSR_{s^*,s,st,so,rm,sk} + \sum_{s^* \in S} \sum_{p \in P^A_{s^*}} OUTP_{s^*,p,cp} SPR_{s^*,s,p,rm,sk} - INR_{s,rm,sk,cp} = 0$$

$$\forall s \in S,\ cp \in CP_s,\ rm \in RM^A,\ sk \in SK_{s,rm} \qquad \text{(A1)}$$

where $PREV_{sk=1} = 0$ and $PREV_{sk \in SK_{s,rm} \setminus \{1\}} = OUTSK_{s,rm,sk-1,cp}(1 - SKP_{s,rm,sk})$.

Outlet mixers of RMX units $mi \in MI^{PRM}_{s,rm}$

$$\sum_{sk \in SK_{s,rm}} OUTSK_{s,rm,sk,cp} SKP_{s,rm,sk} - OUTR_{s,rm,cp} = 0$$

$$\forall s \in S,\ cp \in CP_s,\ rm \in RM \qquad \text{(A2)}$$

Mixers prior to separation task units $mi \in MI^{ST}_{s,st}$

$$\sum_{s^* \in S} \sum_{f \in F^A_{s^*}} FD_{s^*,f,cp} SFS_{s^*,s,f,st} + \sum_{s^* \in S} \sum_{r \in RM^A} OUTR_{s^*,r,cp} SRS_{s^*,s,r,st} + \sum_{s^* \in S} \sum_{sts \in ST^A_{s^*} \setminus \{st\}} \sum_{so \in SO_{s^*,st}} OUTS_{s^*,sts,so,cp} SSS_{s^*,s,sts,so,st} + \sum_{s^* \in S} \sum_{p \in P^A_{s^*}} OUTP_{s^*,p,cp} SPS_{s^*,s,p,st} - INS_{s,st,cp} = 0$$

$$\forall s \in S,\ cp \in CP_s,\ st \in ST_s \qquad \text{(A3)}$$

Network product mixers $mi \in MI^{P}_{s,p}$

$$\sum_{s^* \in S} \sum_{f \in F^A_{s^*}} FD_{s^*,f,cp} SFP_{s^*,s,f,p} + \sum_{s^* \in S} \sum_{rm \in RM^A} OUTR_{s^*,rm,cp} SRP_{s^*,s,rm,p} + \sum_{s^* \in S} \sum_{st \in ST^{A*}_{s}} \sum_{so \in SO_{s^*,st}} OUTS_{s^*,sts,so,cp} SSP_{s^*,s,st,so,p} - OUTP_{s,p,cp} = 0$$

$$\forall s \in S,\ cp \in CP_s,\ p \in P_s \qquad \text{(A4)}$$

Well-mixed cells $sk \in SK_{s,rm}$

$$INR_{s,rm,sk,cp} + \sum_{rx \in RX^A_{s,rm}} \nu_{s,rx,cp} RXR_{s,rx,rm,sk} \frac{\epsilon_{s,rm,sk} V_{s,rm}}{|SK_{s,rm}|} + \sum_{s^* \in S \setminus \{s\}} MTR_{s^*,s,rm,sk,cp} - OUTSK_{s,rm,sk,cp} = 0$$

$$\forall (s \in S,\ sk \in SK,\ cp \in CP) \qquad \text{(A5)}$$

Separation task units $st \in ST_s$

$$\sum_{so \in SO_{s,st}} OUTS_{s,st,so,cp} CD_{s,st,sko,cp} - INS_{s,st,cp} = 0$$

$$\forall s \in S,\ cp \in CP_s,\ rm \in RM \qquad \text{(A6)}$$

For a structure to be feasible, the following equality and inequality constraints associated with the individual splitters must be satisfied

Split fractions associated with splitters $SP^{F}_{s,f}$

$$\sum_{s^* \in S} \sum_{rm \in RM} \sum_{sk \in SK} SFR_{s,s^*,f,rm,sk} + \sum_{s^* \in S} \sum_{st \in ST_{s^*}} SFS_{s,s^*,f,st} + \sum_{p \in P_s} SFP_{s,f,p} - 1 = 0 \quad \forall s \in S,\ f \in F_s \tag{A7}$$

Split fractions associated with splitters $SP^{RM}_{s,rm}$

$$\sum_{s^* \in S} \sum_{rm \in RM} \sum_{sk \in SK} SRR_{s,s^*,r,rm,sk} + \sum_{s^* \in S} \sum_{st \in ST_{s^*}} SRS_{s,s^*,r,st} + \sum_{p \in P_s} SRP_{s,r,p} - 1 = 0 \quad \forall s \in S,\ r \in RM^{A} \tag{A8}$$

$$\sum_{s^* \in S} \sum_{sk \in SK} SRR_{s,s^*,r,r,sk} - 1 < 0 \qquad \forall s \in S,\ r \in RM^{A} \tag{A9}$$

Split fractions associated with splitters $SP^{ST}_{s,st,so}$

$$\sum_{s^* \in S} \sum_{rm \in RM} \sum_{sk \in SK} SSR_{s,s^*,sts,so,rm,sk} + \sum_{s^* \in S} \sum_{st \in ST_{s^*}} SSS_{s,s^*,sts,so,st} + \sum_{p \in P_s} SSP_{s,sts,so,p} - 1 = 0 \quad \forall s \in S,\ st \in ST^{A}_{s},\ so \in SO_{s,st} \tag{A10}$$

$$SSS_{s,s,st,so,st} = 0 \quad \forall s \in S,\ st \in ST^{A}_{s},\ so \in SO_{s,st} \tag{A11}$$

Split fractions associated with splitters $SP^{P}_{s,p}$

$$\sum_{s^* \in S} \sum_{rm \in RM} \sum_{sk \in SK} SPR_{s,s^*,pr,rm,sk} + \sum_{s^* \in S} \sum_{st \in ST_{s^*}} SPS_{s,s^*,pr,st} - 1 = 0 \quad \forall s \in S,\ pr \in P^{A}_{s} \tag{A12}$$

Manuscript received Apr. 22, 2002, and revision received Nov. 25, 2002.